Sensitivity of Vatnajökull ice cap hydrology and dynamics to climate warming over the next 2 centuries

Gwenn E. Flowers,[1,2] Shawn J. Marshall,[3] Helgi Björnsson,[1] and Garry K. C. Clarke[4]

[1] The sensitivity of Vatnajökull ice cap to future climate change is examined using spatially distributed coupled models of ice dynamics and hydrology. We simulate the evolving ice cap geometry, mass balance, velocity structure, subglacial water pressures and fluxes, and basin runoff in response to perturbations to a 1961–1990 reference climatology. For a prescribed warming rate of 2°C per century, simulated ice cap area and volume are reduced by 12–15% and 18–25% within 100 years, respectively. Individual outlet glaciers experience 3–6 km of retreat in the first 100 years and a total retreat of 10–30 km over 200 years. For the same applied warming our results suggest a maximum increase in glacier-derived runoff of ∼25% after 130 years. Ice cap thinning and retreat alters Vatnajökull's subglacial hydraulic catchment structure in the simulations, with up to several kilometers of local hydraulic divide migration. This serves to redistribute water among the major outlet rivers and, in extreme cases, to isolate river basins from glacially derived runoff. Glacier discharge from northern and northwestern Vatnajökull (distal from the coast) appears to be the most robust to climate warming, while discharge from Vatnajökull's southern margin (proximal to the coast) is particularly vulnerable. The latter reflects pronounced changes in the geometry of the southern outlet glaciers and has implications for glacier flood routing and frequency.

1. Introduction

[2] Iceland lies in what is recognized as a climatically important region of the North Atlantic, at the boundary between polar and midlatitude atmospheric circulation cells and oceanic currents. Its position between the warm Irminger and cold East Greenland and East Iceland ocean currents has led to a documented historical sensitivity to changes in ocean circulation [e.g., *Geirsdóttir and Eiríksson*, 1994]. Iceland's glaciers and ice caps, which presently cover approximately 10% of the land surface, are therefore poised to be highly sensitive climate indicators. Vatnajökull, located near the southeast coast of Iceland (Figure 1), is the largest of the country's four major ice caps and is the largest nonpolar ice cap in Europe. Because it is temperate (isothermal at the melting point) and stores much of its mass at low elevation, small changes in air temperature can be expected to have pronounced effects on its geometry.

Precipitation along Iceland's southeast coast is extreme, up to 4 m per year, and Vatnajökull presently discharges around 500 m^3 s^{-1} of water under zero net mass balance conditions [*Björnsson et al.*, 1998]. As such, Vatnajökull is a dynamic conveyor in the hydrologic cycle of southeast Iceland, and regional hydrology would be significantly affected by future climate-induced glacier changes. The position, properties, and configuration of Vatnajökull ice cap make it a valuable scientific resource for understanding local and regional-scale implications of future climate change.

[3] Recent simulations of the National Center for Atmospheric Research Community Climate System Model (NCAR-CCSM) [*Kiehl and Gent*, 2004] suggest roughly 3°C of warming for Iceland by 2140, relative to a 1960–1990 control climatology, in model experiments with a 1% increase in CO_2 per year [cf. *Gent and Danabasoglu*, 2004; B. Otto-Bliesner, personal communication, 2003]. Similar projections have been made by other coupled atmosphere-ocean models [e.g., *Sun and Hansen*, 2003; *Thorpe et al.*, 2001], but the effect of this warming remains to be determined. Realistic glaciological forecasting is clearly important in quantifying the implications of climate warming for Iceland and for other areas at high latitude. In this study we explore the ice cap sensitivity to possible future climates, with an emphasis on ice cap hydrology. This sensitivity manifests itself in glacier runoff magnitude, subglacial discharge routing, and groundwater recharge rate.

[1]Science Institute, University of Iceland, Reykjavik, Iceland.
[2]Now at the Department of Earth Sciences, Simon Fraser University, Burnaby, British Columbia, Canada.
[3]Department of Geography, University of Calgary, Calgary, Alberta, Canada.
[4]Department of Earth and Ocean Sciences, University of British Columbia, Vancouver, British Columbia, Canada.
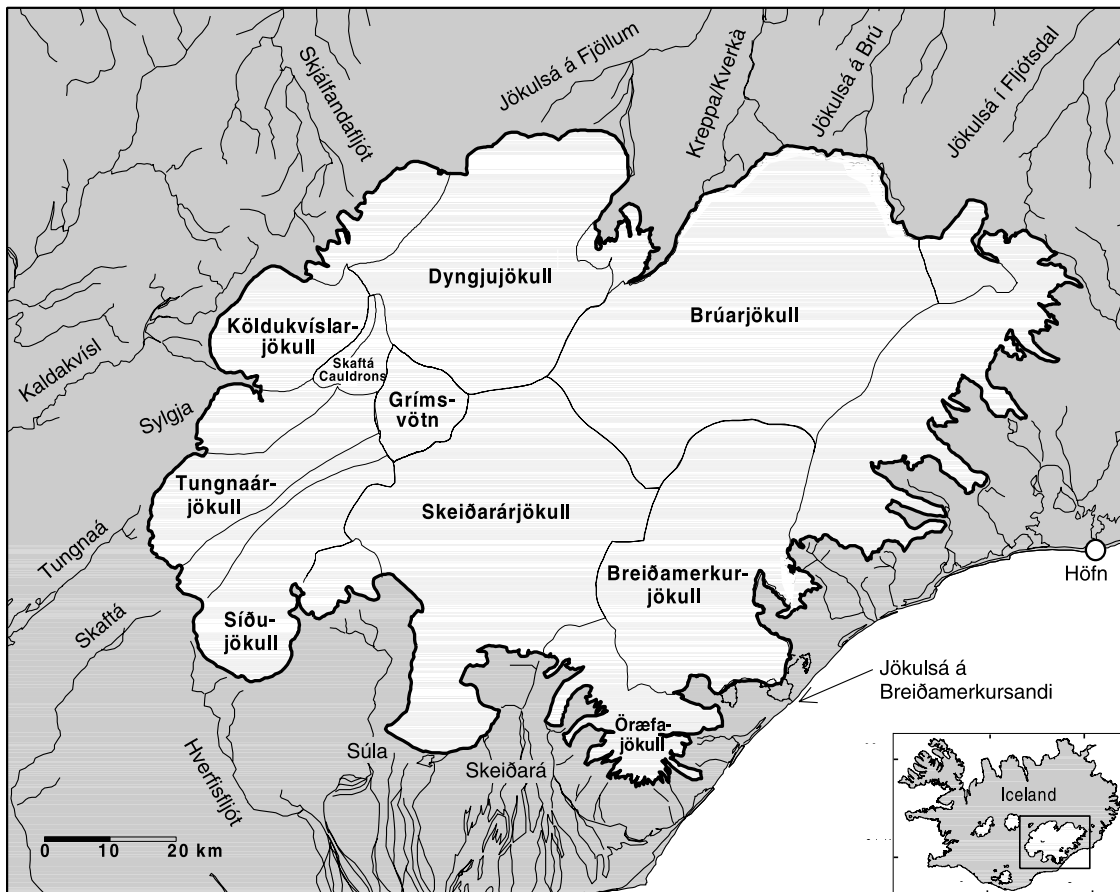
Figure 1. Location map of Vatnajökull and its major outlet rivers. Individual outlet glaciers are delineated by their ice divides.

Changes in these quantities have implications for ice cap dynamics, glacier outburst floods, and river discharge, all of which bear on public works or resource issues for Iceland. We build on prior work to monitor and characterize the geometry, flow regime, hydrology, and dynamics of the ice cap [*Adalgeirsdóttir et al.*, 2000; *Björnsson*, 1982, 1986a, 1986b, 1988, 1998; *Björnsson et al.*, 1998; *Flowers et al.*, 2003] as well as the recent modeling work of *Adalgeirsdóttir* [2003] to begin addressing these issues.

2. Approach

[4] We employ a thermomechanical ice sheet model to derive a glaciologically consistent picture of the evolution of Vatnajökull ice cap geometry and dynamics. This model is asynchronously coupled to a distributed model of glacier hydrology, which requires glacier geometry and rates of surface and basal water supply as input. Among other quantities, the hydrological model computes subglacial water pressures, which are used to define the basal boundary condition for the ice sheet model. Our simulations are initialized with present-day ice geometry and are subjected to a 400 year historical climate spin-up before hypothetical future climatologies are imposed.

[5] Because this study emphasizes the sensitivity of ice cap hydrology to climate change, we strive to generate realistic simulations of the ice cap itself but we do not claim that these simulations represent forecasts. To forecast actual change would require better climate control and more detailed knowledge of glacier mass balance than we aim for at this stage. Hence our emphasis is upon examining the hydrological sensitivity to various climate-induced glacier changes, rather than to perfect our rendering of glacier response to climate. In the sections to follow, we briefly introduce the coupled model equations, discuss the assignment of important parameters, and outline our approach to defining an appropriate model initialization and relevant climate scenarios.

2.1. Ice Dynamics

[6] Ice dynamics are solved using a three-dimensional time-dependent model [*Marshall and Clarke*, 1997a, 1997b; *Marshall et al.*, 2000], built on the standard continuity equations of mass, momentum, and energy. The balance equation for incompressible ice is

$$\frac{\partial h_i}{\partial t} + \nabla \cdot (\bar{v}_i \, h_i) = \dot{b}_i, \tag{1}$$

where h_i is ice thickness, t is time, $\bar{v}_i$ is the vertically averaged velocity, and $\dot{b}_i$ is the mass balance rate. We assume the shallow ice approximation, as deemed appropriate for Vatnajökull by *Adalgeirsdóttir* [2003] and explained further by S. J. Marshall et al. (Simulation of

Vatnajökull ice cap dynamics, submitted to *Journal of Geophysical Research*, 2004, hereinafter referred to as Marshall et al., submitted manuscript, 2004). Ice rheology is described by *Glen*'s [1955] flow law:

$$\dot{\epsilon}_{jk} = B_0 \exp(-Q_i/R\,T_i)\Sigma_2'^{(n-1)/2}\sigma_{jk}', \qquad (2)$$

where $\dot{\epsilon}_{jk}$ is the strain rate, B_0 is the flow law coefficient, $Q_i = 60.7$ kJ mol^{-1} is creep activation energy, $R = 8.314$ J mol^{-1} K^{-1} is the gas constant, T_i is ice temperature, $n = 3$ is the Glen flow law exponent, σ_{jk}' is deviatoric stress, and Σ_2' is its second invariant. The flow law parameter we use, $B_0 = 3.0 \times 10^{-5}$ Pa^{-3} a^{-1}, is taken from an earlier study on Vatnajökull [*Adalgeirsdóttir et al.*, 2000]. The prefactor $B_0 \exp(-Q_i/RT_i)$ in (2) is uniform in our study because Vatnajökull is isothermal.

[7] A sliding rule is adapted from *Payne* [1995] to calculate basal velocity:

$$v_{Bj} = -B_s F \rho_i g h_i \nabla(h_i + z_B), \qquad (3)$$

where B_s is an adjustable parameter that controls the sliding rate, $F = p_w/p_i$ is the ratio of water to ice overburden pressure at the bed, ice density $\rho_i = 910$ kg m^{-3}, $g = 9.81$ m s^{-2}, h_i is ice thickness, and z_B is the elevation of the bed. The spatially distributed quantity F is determined by the hydrology model and is used rather than effective pressure ($p_i - p_w$) in (3) to avoid singularities in the sliding law.

[8] Bed isostasy is accounted for assuming a damped recovery to isostatic equilibrium:

$$\frac{\partial z_B}{\partial t} = -\left(\frac{z_B - z_B^0}{\tau} + \frac{\rho_i\,h_i + \rho_w\,\delta h_w}{\rho_B\,\tau}\right), \qquad (4)$$

with equilibrium bed elevation z_B^0, bed density $\rho_B = 3200$ kg m^{-3}, water density $\rho_w = 1000$ kg m^{-3}, changes in water layer thickness δh_w to account for surface loading due to ice-marginal lakes of depth h_w, and timescale τ taken to be 210 years [*Sigmundsson*, 1991; *Sigmundsson and Einarsson*, 1992]. The equilibrium bed elevation is taken to be $z_B^0 = z_B + (\rho_i/\rho_B)h_i$.

2.2. Mass Balance

[9] The glacier mass balance rate $\dot{b}_i$ in (1), is the difference between ice accumulation and ablation rates, $\dot{a}_i - \dot{m}_i$. Glacier surface mass balance is determined using the annual degree day method [*Huybrechts et al.*, 1991; *Letréguilly et al.*, 1991; *Reeh*, 1991; *Jóhannesson et al.*, 1995], whereby the precipitation fraction deposited as snow and the surface melt are computed from a representation of the annual temperature cycle. This representation assumes sinusoidal variation about the mean annual temperature with an amplitude equal to that of the annual cycle, approximated here as the difference between mean annual and July temperatures. The fraction of precipitation that falls as snow is calculated as a function of this temperature cycle and a threshold below which precipitation falls as rain, often taken as 1°C [*Jóhannesson et al.*, 1995]. The accumulation rate $\dot{a}_i$ is then computed as a function of the precipitation rate, snow fraction, and ice and water densities.

[10] Snow and ice ablation are parameterized as a function of positive degree days (PDD) using the temperature cycle described above. Calculated snow and ice melt rates require different degree day factors (DDFs), which we take as DDF$_{snow}$ = 0.0056 and DDF$_{ice}$ = 0.0077 m water equivalent (w.e.) °C^{-1} d^{-1} from a study of Sátujökull in Hofsjökull ice cap, central Iceland [*Jóhannesson et al.*, 1995]. More recent detailed comparisons of energy balance and degree day models for various outlet glaciers of Langjökull and Vatnajökull ice caps have yielded DDFs in the range of 0.0040–0.0079 m w.e. °C^{-1} d^{-1} for snow and 0.0049–0.011 m w.e. °C^{-1} d^{-1} for ice/firn [*Gudmundsson et al.*, 2003]. For the six Vatnajökull outlet glaciers included in the study, the mean degree day factors were 0.0059 and 0.0075 m w.e. °C^{-1} d^{-1} for snow and ice, respectively, representing differences of 6% and 2% compared to the values of *Jóhannesson et al.* [1995].

[11] Energy loss due to meltwater refreezing in cold snow or at the ice surface is accounted for by specifying a refreezing fraction, which we take as 0.02. This low value reflects observations at Vatnajökull suggesting that the snowpack becomes isothermal within a few days after the onset of surface melting. Details of this surface mass balance treatment are given by *Marshall and Clarke* [1999]. Climate inputs are discussed further in section 2.5.

[12] Detailed studies highlight the complexity of correctly modeling the mass balance of Vatnajökull [*Adalgeirsdóttir*, 2003; *Adalgeirsdóttir et al.*, 2003]. Because of the ice cap orography and its maritime location, climate regimes differ between various sectors of Vatnajökull. The equilibrium line altitude (ELA) varies with position and aspect, and mass balance gradients differ above and below the ELA [*Adalgeirsdóttir*, 2003; *Adalgeirsdóttir et al.*, 2003]. We recognize that our simple treatment of surface mass balance could be problematic given Vatnajökull's evidently complex climate response. However, we are encouraged that our treatment produces ELAs and mass balance distributions that satisfactorily resemble the observations [e.g., *Björnsson et al.*, 1998] when present-day climatology is applied. We submit that this is sufficient to achieve our modeling goal of simulating realistic glaciological behavior, but precludes us from confidently forecasting actual glacier change.

[13] In addition to surface ablation, basal and internal melting contribute to the total ablation rate $\dot{m}_i$, through basal friction, geothermal heating, and strain heating in deforming temperate ice. Assuming internal melt is routed instantaneously to the bed for an isothermal ice cap, we define the basal/internal melt rate $\dot{m}_B$ as the sum of these contributing terms:

$$\dot{m}_B = \frac{1}{\rho_i L}\left(Q_G + v_{Bj}\tau_{Bj} + \Phi_d\Delta z\right), \qquad (5)$$

where $L = 3.34 \times 10^5$ J kg^{-1} is the latent heat of fusion of ice, Q_G is the geothermal heat flux, v_{Bj} is calculated from (3), τ_{Bj} is the basal shear stress, Φ_d is strain heating per unit volume, and Δz is a unit depth.

[14] After substantial model testing we have elected to exclude concentrated geothermal heat sources from this study, such as Grímsvötn and the Skaftá cauldrons, for several reasons: (1) although heat flux is high in these areas, geothermally derived meltwater is a small component of the
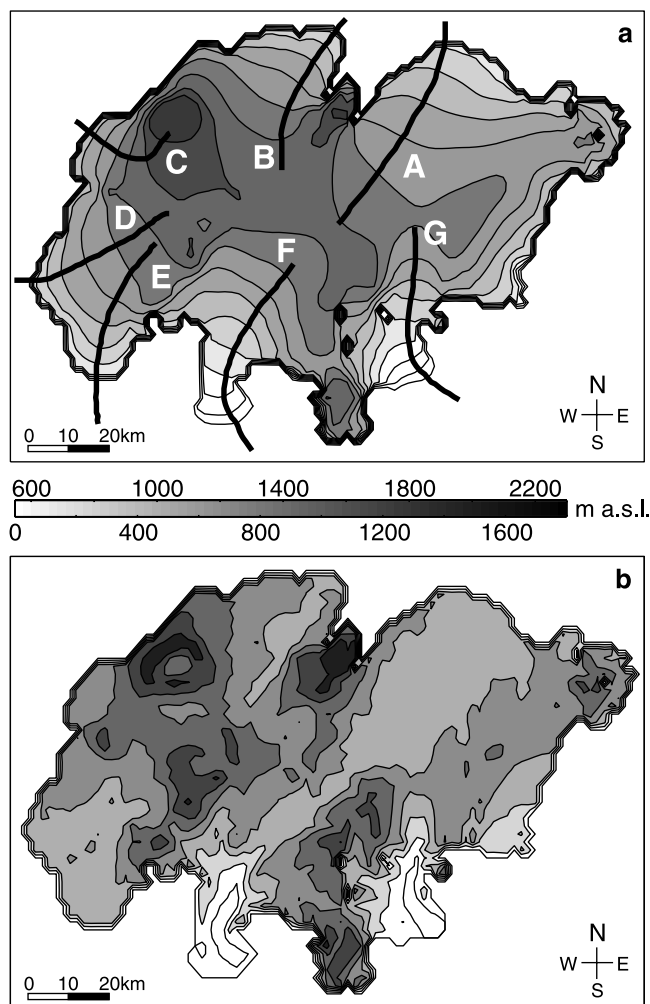
Figure 2. Digital elevation models. (a) Ice surface. Profiles A–G indicate flow lines along major outlet glaciers Brúarjökull, Dyngjujökull, Köldukvíslarjökull, Tungnaárjökull, Síðujökull, Skeiðarárjökull, and Breiðamerkurjökull, respectively. (b) Bed topography.

annual water budget (~5% in 2000 [*Flowers et al.*, 2003]), except during volcanic eruptions which we do not model; (2) while *Aðalgeirsdóttir* [2003] has shown the effect of geothermal heat on ice cap simulations to be substantial on millennial timescales, its impact is much reduced on timescales of several hundred years; (3) geothermally derived meltwater accumulates in subglacial reservoirs which are episodically purged on timescales much shorter than the timescale of interest [see *Björnsson*, 2002], and our model lacks the physics required to simulated these outburst floods; and (4) being highly localized, geothermal heat in areas such as Grímsvötn has ice dynamical impacts that cannot be properly modeled without including longitudinal stresses [*Aðalgeirsdóttir*, 2003], floating ice physics, and a special treatment of subglacial lakes. We apply a uniform background value of $Q_G = 150$ mW m^{-2} beneath the eastern sector of the ice cap. Subsurface hydrothermal circulation beneath western Vatnajökull is thought to be sufficiently vigourous to pump all of the background geothermal heat away from the base of the ice cap (O. G. Flóvenz, personal

communication, 2001). Work by Marshall et al. (submitted manuscript, 2004) addresses key sensitivities of the ice dynamics model as applied to Vatnajökull, including the role of longitudinal stresses and subglacial geothermal heat sources.

[15] When driven by a prescribed climatology and coupled to the bed isostatic model, the ice dynamics model simulates ice cap mass balance, thickness, and internal velocity structure, as well as the evolving land surface geometry. The model is initialized with present-day distributions of ice thickness and bed topography (Figure 2) as explained in Appendix A.

2.3. Hydrology

[16] Subglacial and subsurface water pressures and fluxes are computed with a distributed model of glacier hydrology [*Flowers and Clarke*, 2002a, 2002b] that has been previously applied to characterize the present-day drainage of Vatnajökull [*Flowers et al.*, 2003]. This model consists of two layers, describing water flow at the glacier bed ("subglacial") and in an underlying aquifer ("subsurface"). Surface and basal meltwater are treated as sources to the subglacial drainage system, and water exchange between the subglacial and groundwater systems acts as a source or sink depending on the direction of water flow.

[17] Each system is treated as a vertically integrated layer governed by a local water balance:

Glacier bed

$$\frac{\partial h^s}{\partial t} + \nabla \cdot \bar{Q}^s = \dot{b}_{z_B} + \dot{b}_{z_S} - \phi^{s:a} \tag{6}$$

Aquifer

$$\left(\frac{h^a}{\rho^a}\right)\frac{\partial \rho^a}{\partial t} + \frac{\partial h^a}{\partial t} + \nabla \cdot \bar{Q}^a = \phi^{s:a}. \tag{7}$$

Dependent variables $h^s(x, y, t)$ and $h^a(x, y, t)$ are the local water thicknesses in the subglacial and aquifer systems, respectively. Fluid density in the aquifer $\rho^a = \rho_w \exp (\beta p^a)$, with reference density $\rho_w = 1000$ kg m^{-3}, compressibility $\beta = 5.04 \times 10^{-10}$ Pa^{-1}, and p^a the fluid pressure above a datum $p_0 \approx 0$. Variables $\bar{Q}^s(x, y, t)$ and $\bar{Q}^a(x, y, t)$ are vertically integrated fluid fluxes. Source/sink terms are the basal/internal melt rate $\dot{b}_{z_B}$, the rate of surface water delivery to the bed $\dot{b}_{z_S}$, and subglacial-aquifer water exchange $\phi^{s:a}$. Quantities $\dot{b}_{z_B}$ and $\dot{b}_{z_S}$ are furnished by the ice sheet model, with $\dot{b}_{z_B} = (\rho_i/\rho_w) \dot{m}_B$ where $\dot{m}_B$ is given in (5). Both surface meltwater and precipitation fallen as rain are included in the surface water source term $\dot{b}_{z_S}$. Given the timescales relevant to this study, we assume that all surface water reaches the bed.

[18] As for Darcian flow, we write the vertically integrated subglacial water flux in (6) as

$$\bar{Q}^s = -\frac{K^s h^s}{\rho_w g} \nabla \psi^s, \tag{8}$$

with hydraulic conductivity $K^s = K^s(h^s)$ providing a smooth transition between parameters K^s_{min} and K^s_{max}, and fluid potential $\psi^s = p^s + \rho_w g z_B$, where p^s is water pressure. Mathematical closure requires a relationship for p^s as a function of h^s. We use $p^s(h^s) = p_i(h^s/h^s_c)^{7/2}$ [*Flowers and*
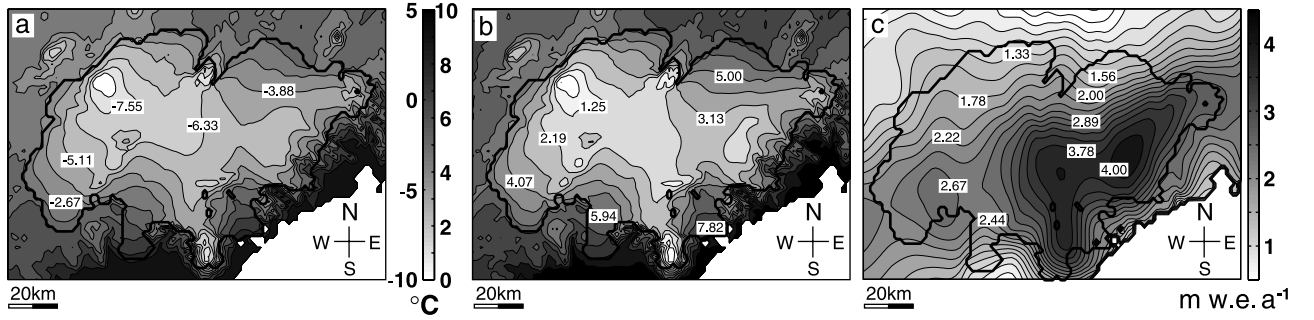
Figure 3. Surface air temperature and precipitation fields. (a) Mean annual surface air temperature T_{ann}^{IMO} from 1961 to 1990. (b) Mean July surface air temperature T_{jul}^{IMO} from 1961 to 1990. Temperature fields are from the Icelandic Meteorological Office and are the basis for our derived reference temperatures. (c) Mean annual precipitation rate after *Eythórsson and Sigtryggsson*, [1971].

Clarke, 2002a], with ice overburden pressure $p_i = \rho_i\, g\, h_i$, ice thickness $h_i = z_S - z_B$, and critical water sheet thickness h_c^s (porosity $\times$ layer thickness) corresponding to buoyancy pressure $p^s = p_i$.

[19] For a depth-independent aquifer porosity n^a, the water thickness in the aquifer h^a is defined as $n^a(z_w - z_L)$, where z_w and z_L are the elevations of the saturated horizon and the lower boundary of the aquifer, respectively. Groundwater flux is written analogously to (8) in terms of h^a as

$$\bar{Q}^a = -\frac{K^a\, h^a}{\rho_w\, g}\, \nabla \psi^a, \qquad (9)$$

with fluid potential $\psi^a = p^a + \rho_w\, g\, z_L$. For the unsaturated case ($h^a < n^a\, d^a$), $p^a = \rho_w\, g\, h^a$, with n^a and d^a the aquifer porosity and thickness, respectively. For the saturated case with aquifer compressibility α^a, $p^a = \rho_w\, g\, h^a + (h^a - n^a\, d^a)/(\alpha^a\, d^a)$ is derived for vertical stresses on an aquifer [see *Freeze and Cherry*, 1979, p. 57] due to changes in water content [*Flowers and Clarke*, 2002a].

[20] Water exchange between the glacier bed and underlying aquifer, $\phi^{s:a}$, depends on fluid potential differences between the two systems. For saturated and unsaturated conditions in the aquifer, respectively,

$$\phi^{s:a} = \begin{cases} \dfrac{K_t}{\rho_w\, g\, d_t}\left[(p^s - p^a) + \rho_w\, g\, d_t\right] & h^a \geq n^a\, d^a \\[2ex] \dfrac{K_t}{\rho_w\, g\, d_t}\left[p^s + \rho_w\, g\, d_t\right] & h^a < n^a\, d^a, \end{cases} \qquad (10)$$

where K_t and d_t are the vertical conductivity and thickness of the debris layer (aquitard) separating the basal hydraulic system from the aquifer.

[21] Given inputs of glacier geometry (z_S, z_B) and surface and basal melt rates ($\dot{b}_{z_S}$, $\dot{b}_{z_B}$), the hydrology model solves simultaneously for h^s and h^a. From h^s, basal water pressure p^s, and hence $F = p^s/p_i$ in (3), can be calculated. This study profits from previous work on present-day Vatnajökull hydrology using the same model [*Flowers et al.*, 2003], where reference parameters were derived for the subglacial and groundwater systems that produced results in best agreement with the data. For the

subglacial horizon, $h_c^s = 1$ m, $K_{min}^s = 10^{-7}$ m s^{-1}, and $K_{max}^s = 1$ m s^{-1}. For the till cap and groundwater aquifer, $K_t = 10^{-9}$ m s^{-1}, $d_t = 1$ m, $n^a = 0.5$, $d^a = 50$ m, $\alpha^a = 10^{-9}$ Pa^{-1}, and $K^a = 10^{-2}$ m s^{-1}.

2.4. Model Numerics

[22] Finite difference approximations are used to discretize the governing equations on identical grids for the ice dynamics and hydrology models. Preserving the validity of the shallow ice approximation, we use grid cells of size 1.62 km $\times$ 1.85 km in the zonal and meridional dimensions, respectively. Both models employ a staggered grid and have variables represented as blended values of their implicit and explicit components (Crank-Nicolson). A Newton-Krylov iterative procedure is used to solve the sparse systems of equations governing ice cap dynamics and hydrology. In most simulations, we use a time step of 0.01 years for the ice dynamics model and update the hydrology every five years. Each time this update occurs, the hydrology model is initialized with its previous solution and run to steady state.

2.5. Climate Inputs and Experiments

[23] Surface boundary conditions for the ice dynamics model are furnished by spatial distributions of mean annual and July air temperatures and the mean annual precipitation rate.

2.5.1. Reference Climatology

[24] We derive our reference temperature fields from mean annual and July surface air temperatures published by the Icelandic Meteorological Office for the period 1961–1990 (Figures 3a and 3b) [*Björnsson*, 2003; *Gylfadóttir*, 2003]. The published fields are kriged interpolations of data from 115 manual and automatic weather stations, concentrated near the coast and sparse in the highland interior [*Björnsson*, 2003]. There is substantial uncertainty and possible systematic error in the reconstruction of temperature over the ice caps themselves, due to the paucity of stations near Vatnajökull, the absence of stations on the ice caps with records of sufficient duration to be used in the interpolation, and the fact that the regression parameters are optimized for the whole of Iceland. Winter temperatures over the ice caps may be reasonably well rendered, while summer temperatures are probably overestimated (H. Björnsson, personal communication, 2003). On the basis of this sugges-

tion, we compute the mean annual and July reference fields $T_{\mathrm{ann}}^{\mathrm{ref}}(x, y)$ and $T_{\mathrm{jul}}^{\mathrm{ref}}(x, y)$ as

$$T_{\mathrm{ann}}^{\mathrm{ref}}(x, y) = T_{\mathrm{ann}}^{\mathrm{IMO}}(x, y) - \Delta T_{\mathrm{ann}} \qquad (11)$$

$$T_{\mathrm{jul}}^{\mathrm{ref}}(x, y) = T_{\mathrm{jul}}^{\mathrm{IMO}}(x, y) - \Delta T_{\mathrm{jul}}, \qquad (12)$$

where $T_{\mathrm{ann}}^{\mathrm{IMO}}(x, y)$ and $T_{\mathrm{jul}}^{\mathrm{IMO}}(x, y)$ are the fields given by the Icelandic Meteorological Office (IMO). Perturbations ΔT_{ann} and ΔT_{jul} are temperature adjustments to the mean annual and July IMO fields ($T_{\mathrm{ann}}^{\mathrm{IMO}}$ and $T_{\mathrm{jul}}^{\mathrm{IMO}}$), respectively, used to obtain more realistic reference temperature fields $T_{\mathrm{ann}}^{\mathrm{ref}}$ and $T_{\mathrm{jul}}^{\mathrm{ref}}$. As previously mentioned, we expect the IMO winter temperatures to be correct and the IMO summer temperatures to be overestimated; assuming the mean annual temperature can be approximated as the average of summer and winter temperatures, the error in the mean annual temperature field should be approximately half that of the July temperature field, and hence we take $\Delta T_{\mathrm{ann}} = \Delta T_{\mathrm{jul}}/2$. This is a crude but necessary adjustment, as climatology is the most important determinant of ice cap size and evolution. Indeed, the raw IMO reference climatology leads to a near complete demise of Vatnajökull ice cap in several hundred years (Marshall et al., submitted manuscript, 2004), supporting Björnsson's suggestion of a warm bias over the ice caps. The determination of ΔT_{ann} is explained in Appendix A.

[25] In order for temperature to vary dynamically in the model with changing ice cap elevation, we first compute sea level equivalent temperature fields by applying a constant lapse rate to the surface temperature reference fields:

$$T_{\mathrm{ann}}^{\mathrm{sl}}(x, y) = T_{\mathrm{ann}}^{\mathrm{ref}}(x, y) - \Gamma z_{\mathrm{S}}(x, y, 0) \qquad (13)$$

$$T_{\mathrm{jul}}^{\mathrm{sl}}(x, y) = T_{\mathrm{jul}}^{\mathrm{ref}}(x, y) - \Gamma z_{\mathrm{S}}(x, y, 0), \qquad (14)$$

where $T_{\mathrm{ann}}^{\mathrm{sl}}(x, y)$ and $T_{\mathrm{jul}}^{\mathrm{sl}}(x, y)$ are, respectively, the sea level equivalent annual and July reference temperature fields, $T_{\mathrm{ann}}^{\mathrm{ref}}(x, y)$ and $T_{\mathrm{jul}}^{\mathrm{ref}}(x, y)$ are the surface temperature reference fields computed in (11) and (12), Γ is the atmospheric lapse rate which we take to be $-0.0053°C$ m^{-1} [Jóhannesson et al., 1995], and z_{S} is the ice surface elevation. Surface temperatures $T_{\mathrm{ann}}(x, y, t)$ and $T_{\mathrm{jul}}(x, y, t)$ for an arbitrary ice geometry can then be computed as

$$T_{\mathrm{ann}}(x, y, t) = T_{\mathrm{ann}}^{\mathrm{sl}}(x, y) + \Gamma z_{\mathrm{S}}(x, y, t) \qquad (15)$$

$$T_{\mathrm{jul}}(x, y, t) = T_{\mathrm{jul}}^{\mathrm{sl}}(x, y) + \Gamma z_{\mathrm{S}}(x, y, t). \qquad (16)$$

[26] Mean annual precipitation (Figure 3c) is digitized from the only existing precipitation map of Iceland [Eythórsson and Sigtryggsson, 1971]. This map includes the orographic effects of Vatnajökull, in particular the local precipitation maximum over Vatnajökull's southeastern sector, which is critical to simulating the ice cap mass balance. Because the precipitation distribution is a complicated function of elevation and distance from moisture sources,

it does not lend itself to a simple elevation-based adjustment as was done for temperature. Improvements to this stationary representation of precipitation are underway by other workers using mass balance measurements to reconstruct multidecadal mean annual distributions of precipitation.

2.5.2. Future Climate Scenarios

[27] In this study, future climate scenarios are defined exclusively in terms of perturbations applied to the air temperature and precipitation fields shown in Figure 3. The suite of climate sensitivity tests we present is selected to illustrate a range of future possibilities and is guided by the suggestions of the Intergovernmental Panel on Climate Change (IPCC) Report [Intergovernmental Panel on Climate Change, 2001] and results of the NCAR-CCSM. The IPCC suggests that warming over the next century in the Nordic countries is likely to fall between 1.4 and 5.8°C, with 3°C being a probable average. Precipitation is much more difficult to constrain, but generally increases with warming and is often prescribed as 5% °C^{-1} [e.g., Jóhannesson et al., 1995]. Recent NCAR-CCSM results suggest a warming of about 3°C over Iceland by 2140, or roughly 2°C per century with respect to a 1960–1990 reference climatology (B. Otto-Bliesner, personal communication, 2004) (see Marshall et al. (submitted manuscript, 2004) for an expanded discussion of the NCAR-CCSM simulations for Iceland).

[28] On the basis of this information, we conduct a suite of tests with warming rates of 0°–4°C per century applied to both reference temperature fields $T_{\mathrm{ann}}^{\mathrm{ref}}(x, y)$ and $T_{\mathrm{jul}}^{\mathrm{ref}}(x, y)$. Each warming test is conducted with precipitation rate increases of 0, 5% and 10% °C^{-1}, although the NCAR-CCSM model results suggest a negligible increase in precipitation for Iceland in its projected climatology. Whether this precipitation falls as rain or snow is determined by air temperature, hence transitions from snow to rain in a warming climate are naturally accounted for in the model. Note that the perturbations to precipitation and temperature are defined relative to the reference climate and should not be interpreted as absolute changes relative to present-day conditions. They may be interpreted as perturbations relative to the adjusted 1961–1990 mean climatology, but further claims depend on how well our adjusted climatology compares to actual present-day conditions.

3. Results and Discussion

3.1. Reference Model

[29] The model preconditioning from 1600–2000 (described in Appendix A) is used to identify a reasonable reference model and to evaluate the uncertainty in our results by comparing simulated and observed characteristics of Vatnajökull. With very few data relative to model parameters, one immediately recognizes this as an underdetermined problem, subject to nonunique solutions. However, we find surprisingly little latitude in the selection of model parameters that produce acceptable results. Figures 4b and 4c show the simulated evolution of ice cap volume and area through the preconditioning period, with $\Delta T_{\mathrm{ann}} = 1.12$ and $\Delta T_{\mathrm{jul}} = 2.24°C$ in (11) and (12) and $B_{\mathrm{s}} = 0.0006$ m a^{-1}, Pa^{-1} in (3) (refer to Appendix A). Final simulated values of both ice cap volume and area, 3166 km^3 and 8189 km^2, respectively, are within one percent of their
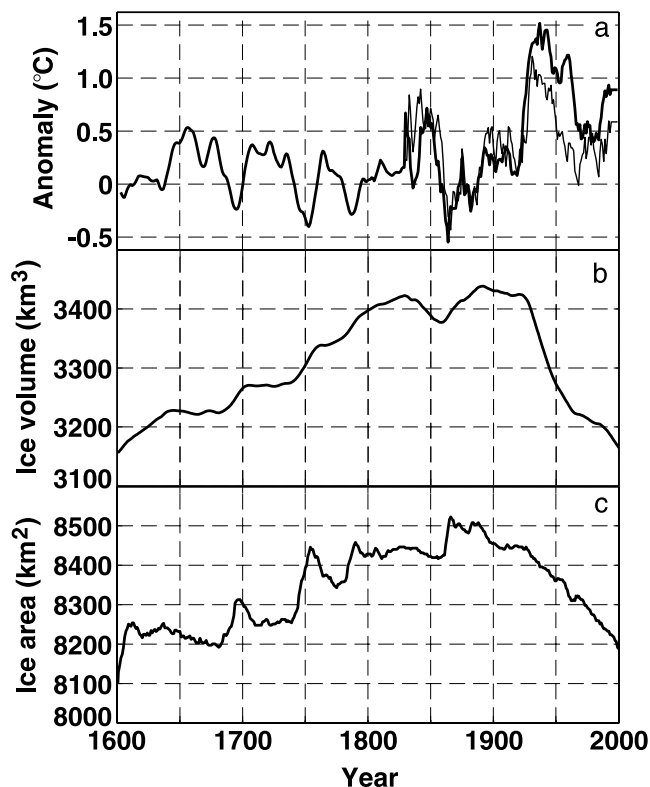
Figure 4. Constructed temperature anomalies and simulated ice cap response to the climate preconditioning. (a) Estimated mean annual (bold line) and mean July (fine line) temperature anomalies relative to 1600 for the period 1600–2000. Record from 1600–1823 is an uncertain estimate based on sea ice cover and other data [*Bergthórsson*, 1969] and is assumed to represent both the annual and July anomalies. Records from 1823–2000 are 11 year running means of measurements from Stykkishólmur, west Iceland. Records before and after 1823 were spliced by shifting them to match their respective means during the interval of mutual overlap from 1823 to 1950. (b) Simulated ice cap volume. (c) Simulated ice cap area.

najökull and intermittently throughout the southeast sector of the ice cap. In a number of locations, the simulated ice extent is significantly less than that observed (arrows, Figure 5). Several areas, such as westernmost Vatnajökull, have a greater simulated than observed ice extent, but this mismatch is small compared to that where the simulated ice extent falls short. The general pattern of mismatch illustrated in Figure 5 is a robust feature of simulations that produced the correct totals of ice volume and area. Hence this pattern can only be improved by spatially selective alteration of the climate fields or heterogeneous tuning of model parameters.

[31] Figure 6 compares simulated and observed glacier geometry along the profiles shown in Figure 2a. These profiles illustrate the problem of differential simulated thinning and thickening between various outlet glaciers, which cannot be cured with homogeneous parameter adjustments. The rate factor B_0 in (2) recommended by *Adalgeirsdóttir et al.* [2000] yields simulated deformational velocities in excellent agreement with minimum observed glacier surface velocities during quiescence (between surges) where data are available (not shown). With our selection of parameter $B_s = 0.0006$ m a^{-1}, Pa^{-1}, simulated surface velocities (deformational plus basal flow) are comparable to or greater than the maximum observed quiescent velocities along the same profiles. This is to be expected for Vatnajökull in order to account for the effect of surges, which occur over about 75% of the ice cap [*Björnsson et al.*, 2003].

[32] There are several reasons for the disagreement illustrated in Figures 5 and 6, aside from simple model inadequacy. As noted by *Adalgeirsdóttir* [2003], the mismatch can be partially attributed to the various outlet glaciers being surveyed in different years, and more importantly, in different phases of their surge cycles. For instance, profiles B, C, and D represent glaciers surveyed in mid-quiescence, while profiles A, F, and G represent those surveyed after a surge. Profile E was surveyed just before a surge. This effect could explain the sign of the error for profiles A, E, and F, as well as the fairly good agreement for profile B, but clearly cannot account for all of the mismatch.
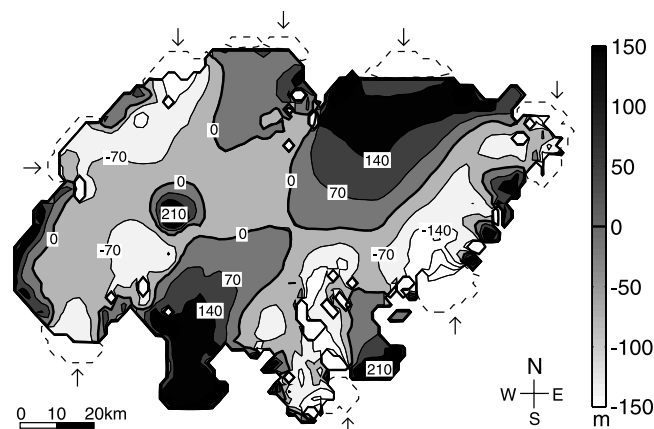
measured values. Note that these curves cannot be interpreted as simulated ice cap histories since we have incorrectly initialized the model with present-day ice geometry. For modest changes in the initial condition, we find the results converge to those shown in Figures 4b and 4c within roughly 100 years (by 1700). However, in using present-day bed topography to initialize the model, no account is taken of changes in bed elevation due to erosion. Trenches observed to be 200–300 m deep beneath the large southern outlet glaciers Skeidarárjökull and Breidamerkurjökull are thought to have been excavated during the Little Ice Age [*Björnsson*, 1996] and could have significant impacts on the historical growth and retreat of these outlets.

[30] Mismatch between simulated and observed present-day ice thicknesses is shown in Figure 5. The nonrandom nature of this error is conspicuous in the simulated thickening of Vatnajökull's largest outlet glaciers, as well as the Grímsvötn area, relative to the observations. Ice that is too thin in the simulations occurs in the central divide area, along a northeast-southwest corridor through western Vat-

Figure 5. Contoured mismatch between simulated and observed present-day ice thicknesses, $h_i^{sim} - h_i^{obs}$. Dotted lines and arrows indicate areas where the simulated ice cap fails to reach the observed present-day ice margin.
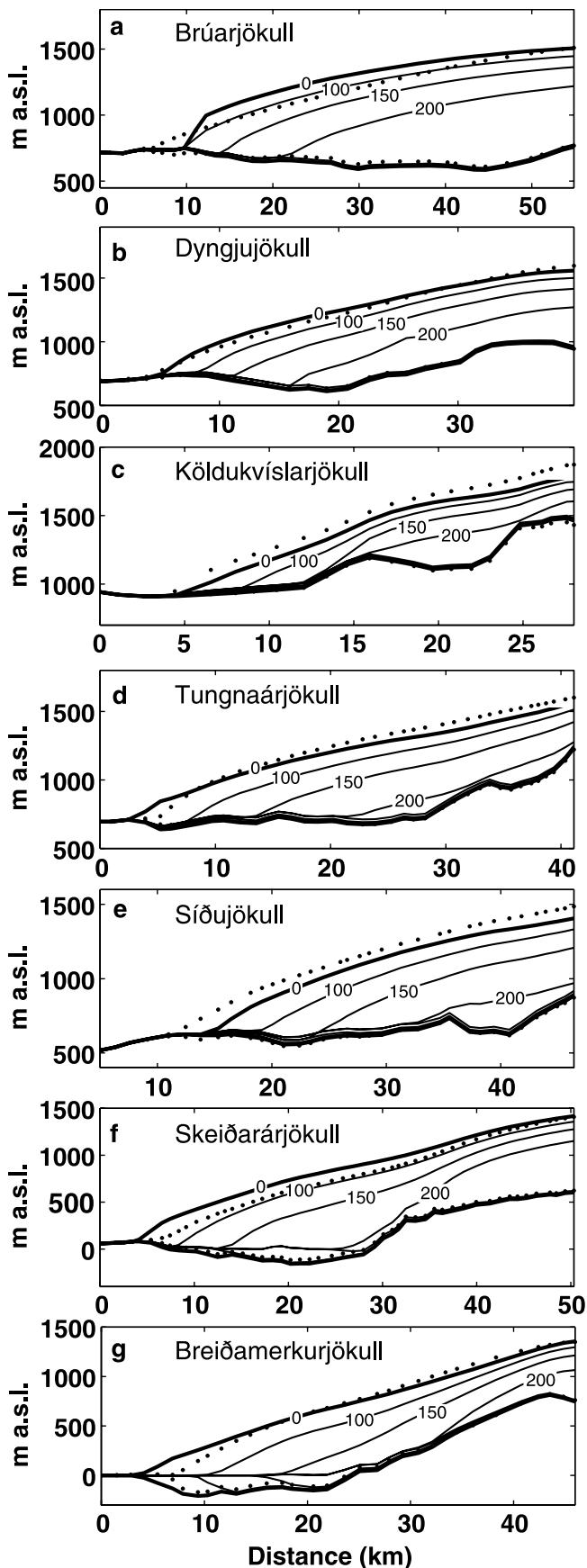
Other factors contributing to our simulation errors include: (1) inaccuracy in the present-day precipitation distribution, (2) past changes in climatology due to historical migration of storm tracks, (3) smoothing of basal topography in the coarse model grid, (4) exclusion of localized geothermal heat sources, (5) use of spatially uniform climate parameters such as DDFs and lapse rate, (6) use of spatially uniform dynamics parameters B_0 and B_s, (7) inability to properly account for glacier surges, (8) neglect of longitudinal stresses, and (9) exclusion of proglacial calving dynamics. Item 4 is clearly responsible for the simulated thickening of the Grímsvötn geothermal area (Figure 5), while 9 must play a role in the simulated overextent of ice along profile G where the glacier front position is controlled by calving into a proglacial lake. Item 3 is likely responsible for some of the thinning in the southeast corridor of the ice cap, where many small and steep outlet glaciers that emerge in narrow valleys are not correctly resolved in the model. The errors in our reference model, illustrated in Figures 5 and 6, provide a guideline for estimating uncertainty in our simulations of Vatnajökull's response to climate change.

3.2. Ice Cap Geometry

3.2.1. Global Variables

[33] Figure 7 shows the simulated evolution of ice cap volume and area in response to $0°–4°C$ per century warming, accompanied by increases in precipitation of $0–10\%\ °C^{-1}$. Each climate scenario is applied to the derived reference climate after the 400 year model preconditioning (Figure 4). Thirteen tests were conducted in total, one with the reference climate held fixed (no warming, curves labeled 0 in Figures 7a and 7b) and three for each warming scenario, with 0, 5, and $10\%\ °C^{-1}$ increases in precipitation (curves labeled 1–4 in Figures 7a and 7b). Each swath in Figure 7 represents the range of solutions for a given warming rate, where the upper bound on the solution corresponds to a $10\%\ °C^{-1}$ precipitation increase and the lower bound to no change in precipitation.

[34] Relative to any of the warming tests, the fixed reference climate simulation produces a fairly stable response in ice cap volume and area. In all tests, volume reduction occurs more rapidly than area reduction. For example, 25% volume loss for $2°C$ per century warming requires roughly 100–120 years (depending on precipitation), while 25% area loss requires 130–150 years for the same warming rate. Area and volume reductions exceed 50% within 200 years for warming rates $\geq 2°C$ per century. Subjected to $4°C$ per century warming, Vatnajökull effectively vanishes within 200 years. Increasing precipitation even by $10\%\ °C^{-1}$ has a minor effect, in this case postponing the disappearance of the ice cap by 20 years.

Figure 6. Profiles of simulated (lines) and observed (dots) glacier surface and bed topography. The bold outermost contours (labeled "0") represent simulated glacier surface profiles for the reference model. Other contours represent simulated glacier surface profiles for 100, 150, and 200 years of $2°C$ per century warming and no change in precipitation. (a–g) Correspond to labels A–G in Figure 2a. Note the difference in horizontal scales between panels.
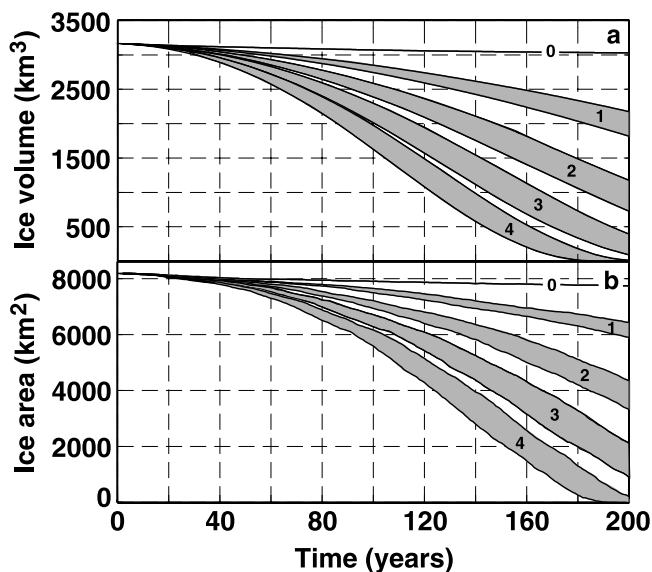
Figure 7. Simulated ice cap response to a warming climate. Shaded areas indicate ranges of solutions for $0-10\%$ °C^{-1} precipitation increase for warming rates of $0°$, $1°$, $2°$, $3°$, and $4°$C per century (labeled 0–4). (a) Ice cap volume. (b) Ice cap area.

3.2.2. Spatial Changes

[35] Figure 8 illustrates the simulated spatial changes in ice cap extent for $1°-4°$C per century warming and no change in precipitation (the latter guided by NCAR-CCSM simulation results). No ice remains after 200 years for $4°$C per century warming (Figure 8d). Test results for warming with increases in precipitation exhibit similar but slightly delayed patterns of ice cap retreat. For instance, the simulated ice cap extent after 200 years for $3°$C per century warming and 10% °C^{-1} precipitation increase lies between those shown for 150 and 200 years in Figure 8c. The retreat patterns in Figure 8b ($2°$C per century warming) are shown for each of the glacier profiles (locations in Figure 2a) in Figure 6.

[36] For any particular total warming, lower warming rates prove more detrimental to ice cap health as they permit more time for the ice cap to equilibrate with the new climate. The result of this is, for example, that Vatnajökull suffers much greater retreat for $4°$C total warming if that warming is applied as $2°$C per century over 200 years rather than $4°$C per century over 100 years. Warming rates of $2°-4°$C per century (Figures 8b–8d) are sufficient to dramatically reduce the ice cap accumulation area. For $2°$C per century warming (Figure 8b), the accumulation area vanishes within 200 years. Consequently, retreat patterns at early times are largely controlled by elevation (with strongly preferential melting at low elevations) and at later times by
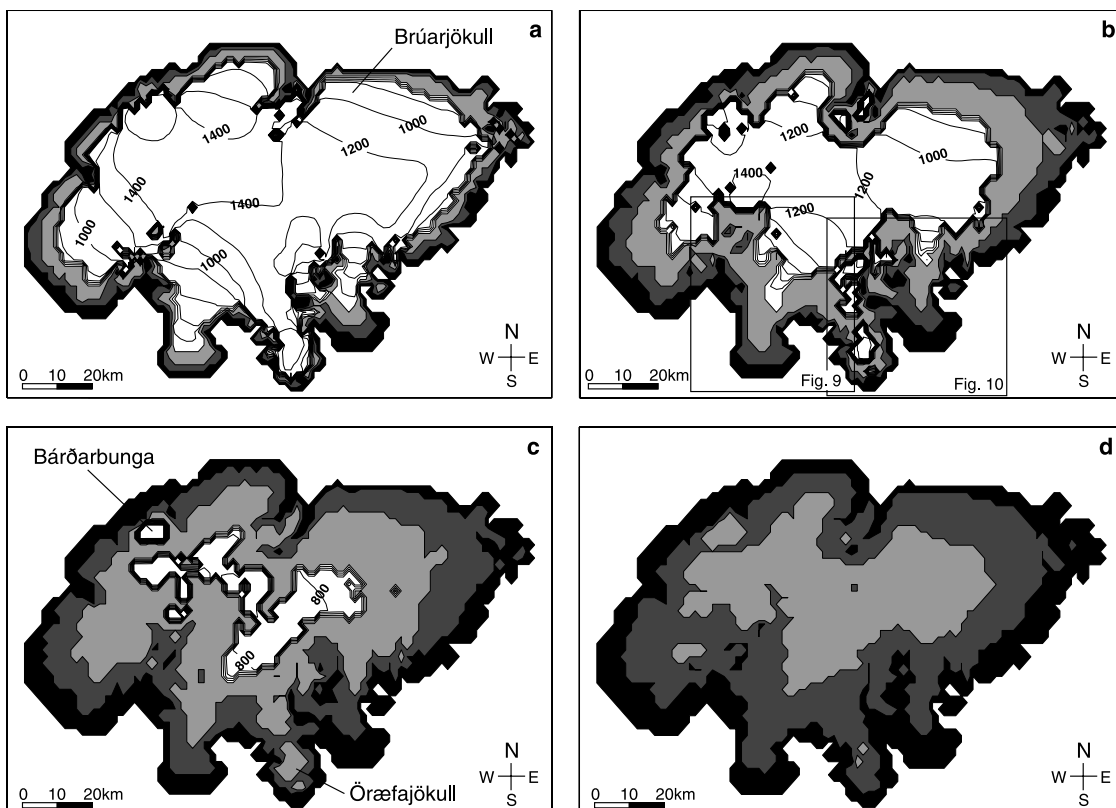

Figure 8. Simulated areal extent of Vatnajökull for the reference model (black) and after 100 (shaded), 150 (lightly shaded), and 200 (white) years of warming with no change in precipitation. Labeled surface contours in Figures 8a–8c indicate the simulated ice surface elevation after 200 years. Per century warming rates are as follows: (a) $1°$C; (b) $2°$C; (c) $3°$C; and (d) $4°$C.

Table 1. Simulated Outlet Glacier Retreat for 2°C Warming Per Century With No Change in Precipitation[a]

Glacier Name	Profile (Figure 2a)	Retreat, km			
		0–100 Years	100–200 Years	(100–200 Years)/(0–100 Years)	0–200 Years
Brúarjökull	A	0	11		11
Dyngjujökull	B	3	8	2–3	11
Köldukvíslarjökull	C	4	7	2	11
Tungnaárjökull	D	5	14	3	19
Sídujökull	E	5	16	3	21
Skeidarárjökull	F	4	17	4	21
Breidamerkurjökull	G	6	22	3–4	27

[a]See Figure 6.

ice thickness. This latter mode, promoted by strong warming and a very diminished or nonexistent accumulation area, produces results such as those in Figure 8c where the ice distribution after 200 years reflects areas of formerly thick ice rather than areas of high elevation.

[37] Although high elevations remain cooler even when there is no accumulation area, thin ice generally occurs on ridges and mountain tops and therefore disappears preferentially under vigorous warming conditions. In our simulations, this produces discontinuous ice along high ridges, for example, leading to isolation of Öræfajökull (Figure 8c, 150 years), and isolation of interior ice-filled calderas such as Bárdarbunga in northwest Vatnajökull (Figure 8c, 200 years). Ice thinning in the vicinity of volcanic centers such as Öræfajökull and Bárdarbunga could have implications for the incidence of volcanic events by altering the subsurface stress regime. Reduced ice load would generally promote surface expressions of volcanic activity, which have the potential to distribute tephra over large areas (reducing the albedo of the ice cap and therefore altering its mass balance for years after an event) and to form subglacial hyaloclastite ridges [see *Gudmundsson et al.*, 1997] and tuyas. Bárdarbunga may have been the eruption site that precipitated the largest glacier outburst floods for which there is evidence in Iceland [see *Björnsson*, 1998; *Björnsson and Einarsson*, 1991], with estimated peak discharges as high as 10^6 m^3 s^{-1} [*Tómasson*, 1973; *Knudsen and Russell*, 2002]. The stratovolcano Öræfajökull was the source of another catastrophic outburst flood in 1362 [*Thorarinsson*, 1958]. Renewed volcanic activity in these ice-filled calderas carries the additional risk of glacier outburst floods occurring in areas where they have been absent for hundreds of years.

3.2.3. Outlet Glacier Retreat

[38] Careful study of Figure 8 reveals that all of Vatnajökull's major outlet glaciers, with the possible exception of Brúarjökull (labeled in Figure 8a), are responsive even to modest climate warming within 100 years. Breidamerkurjökull (G in Figure 2a) and the western outlets Tungnaárjökull and Sídujökull (D and E in Figure 2a) exhibit more rapid retreat rates than Dyngjujökull and Skeidarárjökull (B and F in Figure 2a). With 2°C per century warming, Breidamerkurjökull (Figure 6g), Tungnaárjökull (Figure 6d), and Sídujökull (Figure 6e) retreat ~6, 5, and 5 km, respectively from their reference model profiles (solid lines labeled 0) in 100 years. Dyngjujökull (Figure 6b) and Skeidarárjökull (Figure 6f) retreat ~3 and 4 km, respectively, in the same period, while Brúarjökull exhibits no retreat at all (Figure 6a). Flow line profiles have been interpolated in

order to estimate outlet retreat (see Table 1), and reported retreat rates are rounded to the nearest kilometer to reflect the uncertainty associated with a coarse model grid.

[39] For 2°C per century warming, simulated glacier retreat rates from 100–200 years are roughly two to four times greater than those for 0–100 years. Several factors contribute to this accelerated retreat rate, including increased warming (up to 4°C relative to the reference climate by 200 years, as compared to 2°C after 100 years for a warming rate of 2°C per century), lowered ice surface profiles, and in some cases, adverse bed slopes beneath retreating outlet glaciers. Simulated retreat between 100 and 200 years is highest for the three southern outlets: Breidamerkurjökull (22 km), Skeidarárjökull (17 km) and Sídujökull (16 km), representing threefold to fourfold retreat rate increases relative to the period 0–100 years. The northwestern outlets Köldukvíslarjökull and Dyngjujökull fare best with retreat rates doubling or tripling to yield 7 and 8 km of retreat, respectively from 100–200 years. Brúarjökull and Tungnaárjökull show 11 and 14 km of retreat, respectively, from 100–200 years.

[40] The simulated retreat summarized in Table 1 is computed relative to the reference model, which differs from the measured glacier surface as previously discussed (Figures 5 and 6). In light of the differences between modeled and measured reference profiles, the retreat rates reported in Table 1 may be underestimated for Brúarjökull, Tungnaárjökull, Skeidarárjökull, and Breidamerkurjökull. The opposite is true for Sídujökull where the retreat rate is probably overestimated. Simulated retreat rates for Dyngjujökull are likely to be the most reliable, based on the good agreement between modeled and measured reference profiles (Figure 6b).

[41] For outlets terminating in proglacial lakes, neglecting the calving process further underestimates the retreat rate by excluding an important mass wastage mechanism. This would be true for all outlets with undrained adverse bed slopes at some point during their retreat, most notably Breidamerkurjökull [cf. *Björnsson et al.*, 2001] and Skeidarárjökull in these simulations. While these two outlets retreat past their overdeepenings within 200 years in the simulation shown in Figure 6, the northern outlets Dyngjujökull and Brúarjökull have not yet reached their respective bed minima. For Brúarjökull, this point lies over 35 km upglacier from the present-day terminus yielding potential for a large but shallow proglacial lake at some point in the future (see Figure 6a).

[42] Surges present a complication in relating simulated glacier retreat to actual glacier front position. The reference model was tuned to produce good agreement between
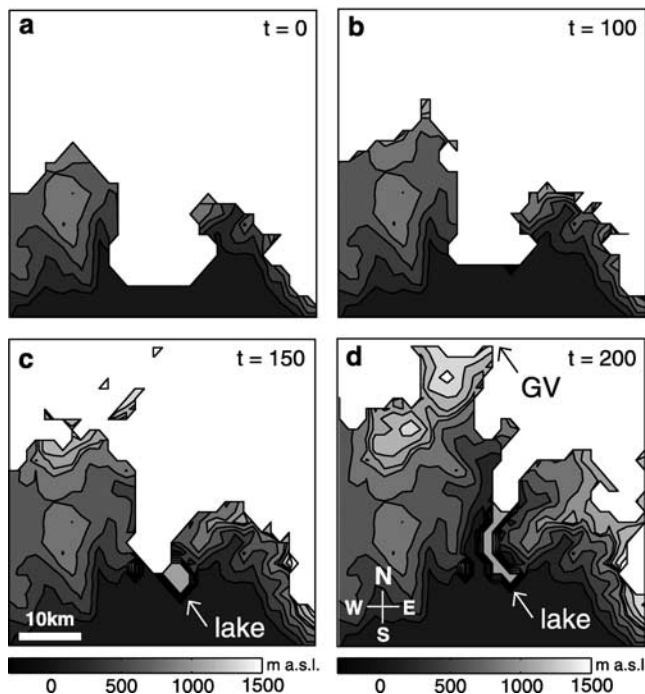
Figure 9. Retreat of Skeidarárjökull in response to 2°C per century warming. Land surface topography is contoured and shaded in each panel, and ice extent is shown in white. (a) Reference model. (b) 100 years. (c) 150 years. (d) 200 years. GV, Grímsvötn subglacial lake. A proglacial lake is shown in Figures 9c and 9d.

3.2.4. Southern Outlet Glaciers

[44] Some of the most dramatic climate-related changes are expected along the southern margin of Vatnajökull. Figures 9 and 10 illustrate this point with the simulated evolution of Skeidarárjökull and Breidamerkurjökull for 2°C per century warming, from which we can interpret secondary hydrological impacts of climate change. At present, water is discharged in a semidistributed fashion from the terminus of Skeidarárjökull, creating the braided river system that crosses Skeidarársandur. Figure 9c shows the glacier retreating after 150 model years into a bedrock trough, which is over 150 m below sea level. This trough would sustain a proglacial lake similar to present-day Jökulsárlón in front of Breidamerkurjökull. The emergence of such a lake is visible in Figure 9c, with its shape governed by the evolving isostatic rebound (compare Figure 9d). Drainage beneath the narrowing ice tongue would be increasingly focused into the bedrock trench emerging from the eastern margin of the glacier at 150 years. The modeled patterns of basal water flow (not shown) and deglaciation in this area suggest that the braided rivers of Skeidarársandur (fed by discharge distributed across the present-day margin of Skeidarárjökull) may collapse into a single very large river, most likely occupying the present-day course of Skeidará.

[45] After 200 years of retreat, the terminus of Skeidarárjökull bifurcates into two distinct branches occupying topographic troughs (Figure 9d). With this geometry, outburst floods from subglacial lake Grímsvötn (GV) would emerge from the northern branch. Though the initiation mechanism for these floods is not fully understood, it is
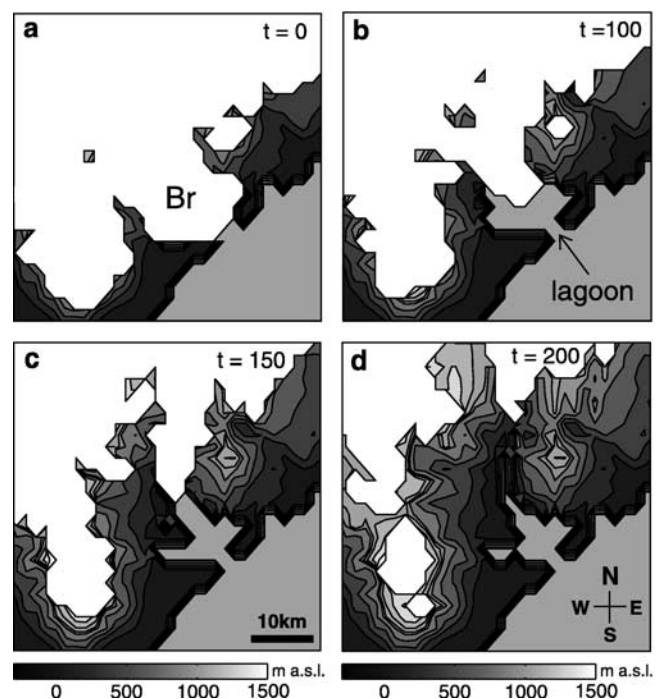
simulated and observed present-day ice thickness and area, which necessitated a high basal flow coefficient to account for the effect of surges. Our simulations of ice cap evolution therefore represent only low frequency or background changes, and cannot capture the high-frequency fluctuations typical of surges. Simulated glacier retreat rates should then be lower than actual retreat rates during glacier quiescence and greater than those during surges.

[43] The picture that emerges for Vatnajökull from these simulations is a geographically organized climate sensitivity, emerging shortly after 100 years of warming. From 100 to 200 years for 2°C per century warming, the northwest sector of the ice cap experiences the least retreat, followed by the northeast (Brúarjökull). The southern outlets undergo the greatest retreat followed by the southwestern and western outlets. Interestingly, the outlet glaciers can be neatly clustered based on their total simulated retreat after 200 years for 2°C per century warming: 11 km for the northern and northwestern outlets Brúarjökull, Dyngjujökull and Köldukvíslarjökull, 19–21 km for the southwestern outlets Tungnaárjökull, Sídujökull and Skeidarárjökull, and 27 km for the southeastern outlet Breidamerkurjökull (see Table 1). The most sensitive of these glaciers are the closest to the coast, experiencing the warmest annual temperatures and the highest rates of precipitation. The more robust glaciers of Vatnajökull's northwest sector, aside from being further interior, are characterized by hypsometric distributions weighted toward high elevations. Both Dyngjujökull and Köldukvíslarjökull tap into the large northwestern ice dome Bárdarbunga.

Figure 10. Retreat of Breidamerkurjökull in response to 2°C per century warming. Land surface topography is contoured and shaded in each panel, and ice extent is shown in white. (a) Reference model. Br, Breidamerkurjökull outlet glacier. (b) 100 years. (c) 150 years. (d) 200 years.
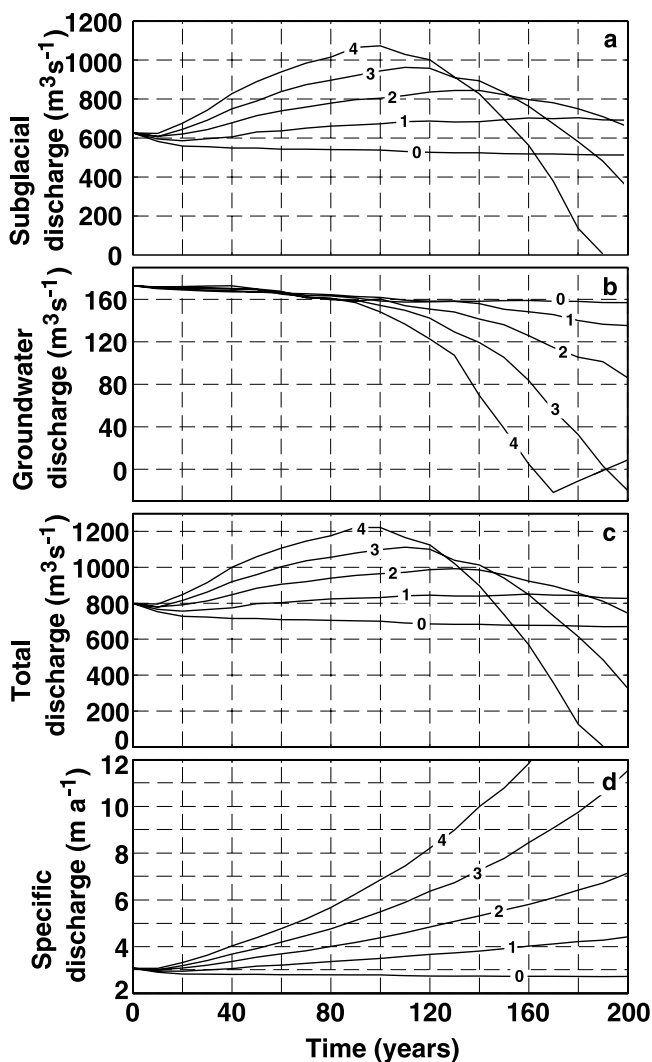
Figure 11. Simulated response of glacier-derived discharge to warming rates of 0°–4°C per century (curves labeled) applied to the reference climate with no change in precipitation. Discharge values represent simulated water fluxes integrated along the ice margin. (a) Subglacial (ice-bed interface) discharge. (b) Groundwater (subsurface) discharge. Negative values indicate net flow toward the ice cap interior. (c) Total discharge (sum of Figures 11a and 11b). (d) Total discharge normalized by ice cap area.

related to the thickness of the ice dam [*Björnsson*, 1974]. Thus as the ice thickness and geometry change in the vicinity of Grímsvötn, changes in glacier flood frequency and magnitude can be expected. In Figure 9d, the ice dam is almost breached by the glacier margin, in which case continuous drainage from Grímsvötn would replace episodic outburst floods. Subglacial outburst floods from ice-marginal lake Grænalón on the western side of Skeidarárjökull (not shown) would also be affected by altered glacier geometry. As the glacier tongue narrows, Grænalón would enlarge, until it eventually established a permanent drainage route along the western margin of Skeidarárjökull.

[46] Figure 10 shows a similar progression in the vicinity of Breidamerkurjökull. The initial extent of both Breidamerkurjökull and Skeidarárjökull is overestimated by the

reference model, hence the present-day lagoon Jökulsárlón is almost absent in Figure 10a. As Breidamerkurjökull thins and retreats, nunataks form (Figure 10b) and ice flow around the largest nunatak eventually fails to reconverge. Breidamerkurjökull retreats as a narrow ice tongue in its deeply excavated valley. The size of the proglacial lagoon is determined by the balance between increasing areal exposure by the retreating glacier and decreasing area below sea level due to isostatic uplift. The extent of the lateral branches of the lagoon is exaggerated in Figures 10b–10d due to the overestimated thickness and extent of Breidamerkurjökull in the reference model.

3.3. Ice Cap Hydrology
3.3.1. Global Variables

[47] Figure 11 summarizes the climate response of Vatnajökull hydrology to warming of 0°–4°C per century and no change in precipitation. Discharge is computed by integrating the simulated water flux around the ice margin. The timing and magnitude of peak discharge is a function of the rate of climate warming. The reference climate held fixed produces a monotonic decline in all discharge quantities (curves labeled 0), while all of the climate warming tests produce discernible peaks in subglacial and total discharge (Figures 11a and 11c). These peaks reflect enhanced melting as well as precipitation that falls as rain and is routed through the glacier. The latter becomes an increasingly important component of runoff as the equilibrium line retreats upglacier and rain replaces snow as precipitation. Timing of peak total discharge (Figure 11c) occurs at approximately 180, 130, 110, and 100 years for warming rates of 1°, 2°, 3°, and 4°C per century, respectively. Maximum total discharge (Figure 11c) exceeds the reference value (at time 0) for these warming scenarios by 6%, 24%, 39%, and 53%, respectively.

[48] Climate-driven changes in Vatnajökull hydrology are concentrated in the subglacial horizon, especially within the first 100 years. This can be attributed to the significantly higher transmissivities of the subglacial drainage system as compared to the groundwater aquifer. Groundwater discharge across the ice margin (Figure 11b) is relatively stable in the first 100 years, reflecting an approximate balance between glacier-derived recharge and a background decline in groundwater flux initiated before time zero. Between 100 and 200 years, the marked decline in groundwater flux across the ice margin is driven by decreased ice cap area, and hence diminishing recharge. With 4°C warming per century, groundwater flow across the ice margin reverses direction (indicated by negative values of discharge in Figure 11b), indicating subsurface water flow toward the ice cap interior from outside the ice margin. The evolution of glacier-derived groundwater recharge (not shown) qualitatively resembles subglacial discharge (Figure 11a). Specific discharge (Figure 11d) increases monotonically in all cases except for the fixed reference climate scenario. Discharge values in Figure 11 are slightly underestimated because geothermal hot spots have not been included in the simulations. As it stands, computed basal melt rates are small and are in many places negligible compared to surface melt rates. Including geothermal heat sources would subject only ~2% of the original glacier bed to basal melt rates comparable to those at the surface.
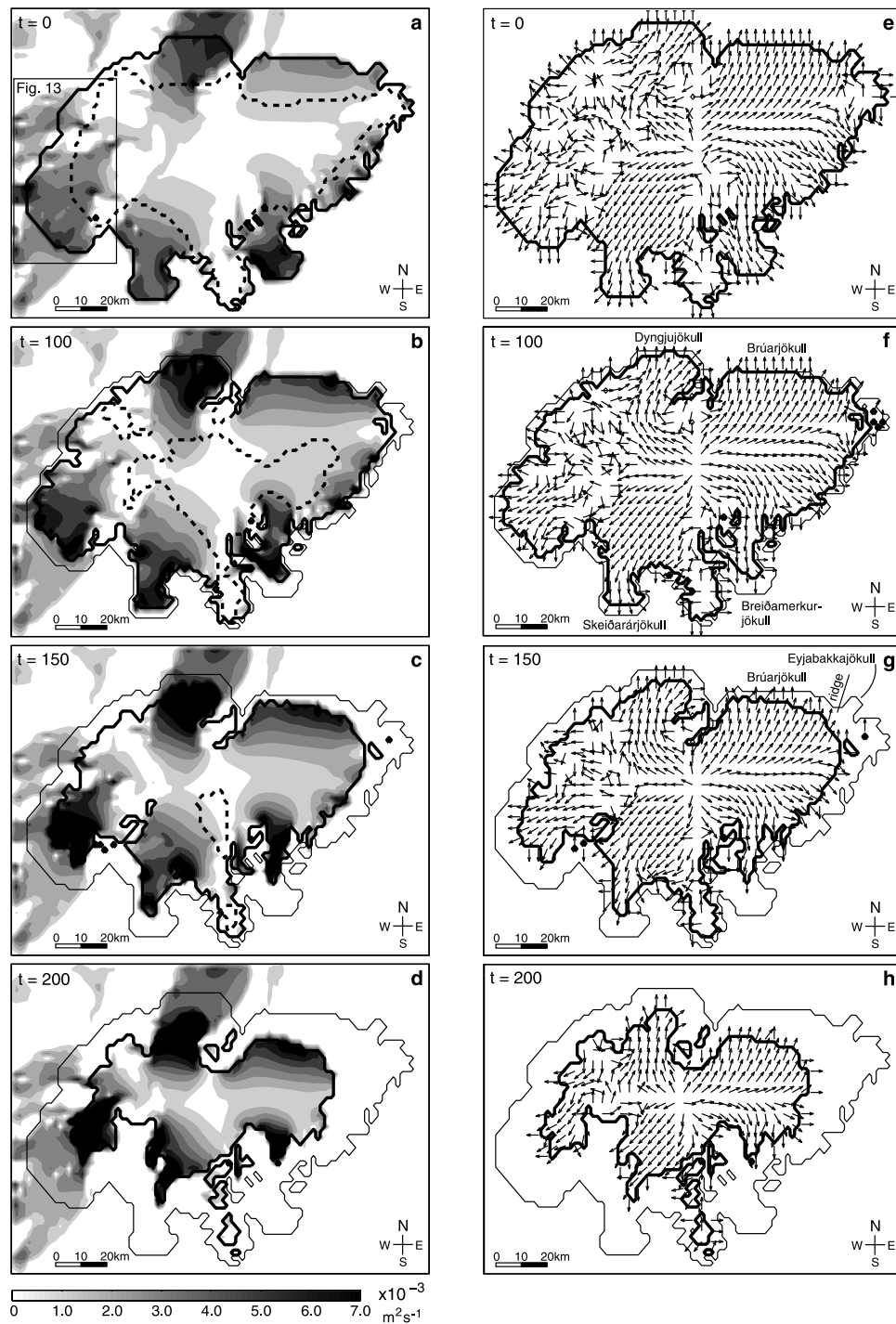
Figure 12. Simulated response of subglacial and subsurface hydrology to 2°C per century warming and no change in precipitation for the (a, e) reference model and for (b, f) 100, (c, g) 150, and (d, h) 200 years. (left) Sum of subglacial and subsurface flux magnitudes, computed as grid cell averages (1.62 × 1.85 km). (right) Simulated flow directions for the subglacial horizon only (sparsely sampled for visual clarity). Reference model ice cap extent is shown as a fine line in each panel; ice cap extent at individual time slices is shown in bold. Accumulation area is shown as a dashed line in Figures 12a–12c. There is no accumulation area in Figure 12d.

3.3.2. Spatial Changes in Ice Cap Drainage

[49] Figure 12 illustrates the simulated spatial changes that accompany warming of 2°C per century with no change in precipitation. We focus our analysis on this particular test as it best represents NCAR-CCSM simulation results for Iceland up to 2140. Panels in the left column of Figure 12 show the sum of subglacial and subsurface flux magnitudes. Active groundwater drainage only takes place beneath the

northwest sector of Vatnajökull, hence this is the only area where simulated water flux appears outside the ice cap footprint. Panels in the right column of Figure 12 illustrate water flow directions in the subglacial horizon only. Sensitivity tests have shown that our choice to allow surface water to penetrate the bed both above and below the equilibrium line has little impact on the simulation results, especially for situations with a rapidly disintegrating accumulation area. By contrast, including rain in the surface water flux to the bed has a marked effect on simulated basal hydrology.

[50] Comparing flux magnitudes in Figures 12a–12d illuminates several trends. Total drainage beneath the ice cap intensifies over time, as indicated by the darkening of shaded areas and the increasing shaded fraction of the glacier bed. After 100 years (Figure 12b) high values of water flux are generally confined to discrete patches of the drainage system close to the ice margin. By 150 years (see Figure 12c), these patches have grown to include a large fraction of several of the outlet glaciers, namely Dyngjujökull in the northwest, the southwestern outlets, and the remnant of Breidamerkurjökull. The southeastern flank of the ice cap, east of Breidamerkurjökull, is the only sector that exhibits a decrease in drainage intensity from 100 to 200 years. This area is separated from the rest of the ice cap by a bedrock ridge roughly parallel to the present-day ice margin. With sufficient ice retreat, settlements such as Höfn (see Figure 1) along the southeast coast of Iceland would be isolated from glacier-fed runoff. Although this eventuality is not realized in the simulation shown in Figure 12, evidence for severely diminished drainage accompanying retreat of Vatnajökull's southeastern flank can be discerned from Figures 10c and 10d.

[51] Simulated subglacial flow direction vectors (Figures 12e–12h) give an indication of evolving drainage patterns beneath the ice cap. Owing to the exclusion of geothermal heat sources, the simulated water flow directions are unreliable in the immediate vicinity of geothermal areas. This primarily affects Grímsvötn in west central Vatnajökull where flow vectors should be turned inward. The model grid is sufficiently coarse that changes in subglacial hydraulic catchment structure can only be interpreted in hydrologically simple environments where bed topography is adequately resolved. This unfortunately excludes west central Vatnajökull where outburst floods originate and several volcanic eruptions have taken place in the last decade [see Björnsson, 2002]. As evidenced in Figures 12e–12h, there is a slight alteration of simulated subglacial catchment structure toward a quadruple divide in the center of the ice cap. This divide structure is in place after 100 years but the quadruple point migrates west 1–2 km by 150 years and a further 4–5 km west by 200 years. North-south hydraulic divide fluctuations of ∼2–6 km in 100 years occur in the simulations between Skeidarárjökull and Dyngjujökull and between Brúarjökull and Breidamerkurjökull (labeled in Figure 12f). This evolution effectively reduces the maximum southern extent of the northern catchment basins. The Skeidarárjökull catchment expands to the north but is eroded to the east 3–4 km by the expansion of Breidamerkurjökull between 150 and 200 years.

[52] With ice thinning and retreat, bedrock ridges develop into hydraulic barriers at various locations around Vatnajö-kull including the previously mentioned southeast sector. For example, the ridge separating Brúarjökull and Eyjabakkajökull (Figure 12g) divides their respective outlet rivers, Jökulsá á Brú and Jökulsá á Fljótsdal (see Figure 1), and serves to isolate Jökulsá á Fljótsdal from Vatnajökull after about 170 simulation years. Kreppa and Kverká, rivers originating from western Brúarjökull and eventually joining Jökulsá á Fjöllum (originating from Dyngjujökull), are similarly cut off from their glacially derived surface water source by 200 years in the simulation. At that point, all ice-marginal discharge from Brúarjökull is routed to Jökulsá á Brú. Under present-day conditions, this could increase the discharge of Jökulsá á Brú by 30% [Flowers et al., 2003].

[53] Figure 13 presents a more detailed picture of the simulated evolution of subglacial and groundwater flow for western Vatnajökull. This sector of Vatnajökull is economically important as the source of several large rivers dammed for hydropower. Western Vatnajökull is underlain by several bedrock ridges trending roughly southwest-northeast, some of which are not well resolved by the model. Despite this, the effect of bed topography can be identified in the subglacial flow field for the reference model (Figure 13a). Owing to the presence of the groundwater system, the glacier bed in this area is relatively well drained. As a consequence, simulated water pressures at the bed are comparatively low, resulting in fluid potential gradients that are sensitive to bed topography. This gives rise to the small-scale variations in flow direction seen in Figure 13a. Simulated flow fields in Figures 13b–13d exhibit better alignment under the southwest lobe of the ice cap, where vigorous surface melting ultimately leads to high water pressures at the bed. These pressures give rise to a flow field dominated by the ice surface slope and much less sensitive to bed topography. In contrast, the groundwater flow field in Figures 13e–13h is more consistently aligned. Water pressure fluctuations in the groundwater system are much smaller than those in the drainage system at the ice-bed interface.

[54] The present-day margin of Tungnaárjökull outlet glacier (labeled, Figures 13a and 13b) is perched on the crest of a bedrock sill (labeled, Figures 13b and 13f), which in the simulations, is exposed by glacier retreat. The river Tungnaá (see Figure 1) is supplied by groundwater upwelling through highly porous basalt conduits and by surface runoff from Vatnajökull. Our simulations suggest that once Tungnaárjökull retreats from this sill (as it has after 100 years in Figure 13b), water emerging from the glacier margin would drain southward rather than westward. Tungnaá would continue to be supplied by groundwater (Figure 13f) after being isolated from Vatnajökull surface runoff. This would diminish the glacially derived component of Tungnaá discharge by 30–80% [Flowers et al., 2003].

[55] Our simulations suggest another example of water rerouting between 150 and 200 years at the northwest margin of the ice cap (black arrow, Figure 13d). Subglacially derived runoff diminishes with ice retreat toward the Bárdarbunga caldera, and after 200 years, reverses direction to flow toward the ice cap interior (Figure 13d). This flow reversal would terminate the glacially derived surface water supply to Skjálfandafljót, a river draining northwest from Bárdarbunga (see Figure 1). Like Tungnaá, the river would continue to be fed by groundwater for a time, but

Figures 13g and 13h suggest progressively weaker groundwater flow in the area as glacial recharge decreases. Other such water reroutings have been suggested as implications of ice cap retreat, including possible redirection of floodwater from the Skaftá cauldrons. Grid resolution precludes

us from making any conclusive statements about flood rerouting with this model.

3.3.3. Changes in Basin Discharge

[56] Drainage intensity beneath different outlet glaciers in Figures 12a–12d provides a qualitative indication of water partitioning between various catchment basins. Figure 14 quantifies the changes in total ice cap discharge (subglacial and groundwater) by glacier catchment for 2°C per century warming and no change in precipitation. Figure 14a gives an indication of the climate-induced variability of basin discharge for each catchment. Brúarjökull and Dyngjujökull drainage basins experience the most significant relative increases in discharge with climate warming, with discharge from the Brúarjökull basin doubling after 150 years. Dyngjujökull is the only basin to experience a monotonic increase in discharge over the 200 year simulation period. Western Vatnajökull, Skeidarárjökull, and Breidamerkurjökull drainage basins undergo smaller relative fluctuations than the northern basins. The combined outlet glaciers of Vatnajökull's southeastern flank display a monotonic decline in total discharge throughout the simulation. Changes in basin discharge are determined by the combined effects of diminishing catchment area due to ice margin retreat, increasing surface meltwater production, and the migration of interior hydraulic divides.

[57] Figure 14b presents the fraction of total runoff from Vatnajökull discharged by each basin for the reference model (t = 0) and for 100, 150, and 200 years. In the simulations, the relative contributions of the represented basins are reorganized such that in 200 years, Brúarjökull and Dyngjujökull carry 35% of the discharge between them, representing a 10% increase relative to the reference model. Breidamerkurjökull's contribution is reduced by 9% over 200 years to be 5% of total discharge, while the western outlets and Skeidarárjökull discharge about 15% and 13%, respectively, down from 20% and 18% initially. With the exception of the southeastern outlets, the significance of Vatnajökull drainage basins after 200 simulated years decreases counterclockwise around the ice cap beginning with Brúarjökull in the northeast.

3.3.4. Basal Dynamics

[58] Ice cap hydrology and dynamics are mutually affected by climate warming. In this coupled model, hydrology impacts ice dynamics through basal sliding as parameterized in (3). A positive feedback cycle has been proposed whereby elevated surface temperatures boost meltwater production, raising subglacial water pressures which facilitate basal motion, resulting in mass transport to lower elevations, and thus accelerating glacier retreat. Our simulations suggest that this type of meltwater feedback has
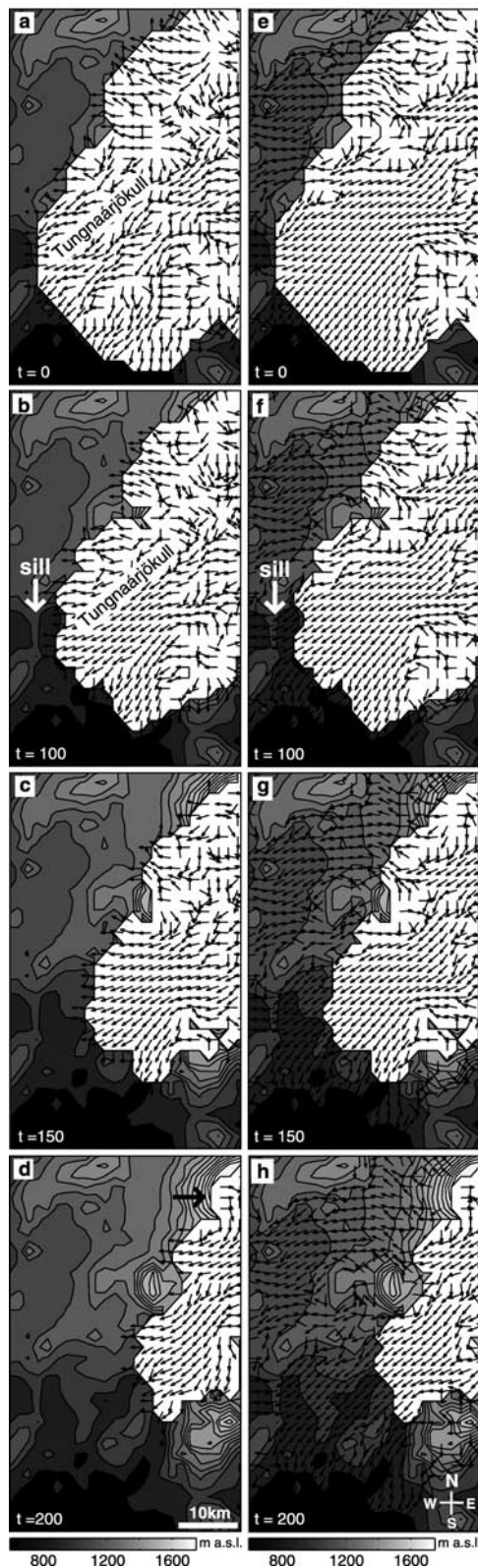
Figure 13. Simulated response of subglacial and subsurface hydrology of western Vatnajökull to 2°C per century warming and no change in precipitation for the (a, e) reference model and for (b, f) 100, (c, g) 150, and (d, h) 200 years. Land surface topography is contoured and shaded in each panel and ice extent is shown in white. (left) Subglacial water flow direction. (right) Groundwater (subsurface) flow direction. White arrows in Figures 13b and 13f indicate a bedrock sill. The black arrow in Figure 13d indicates the ice margin at the Bardabunga caldera rim.
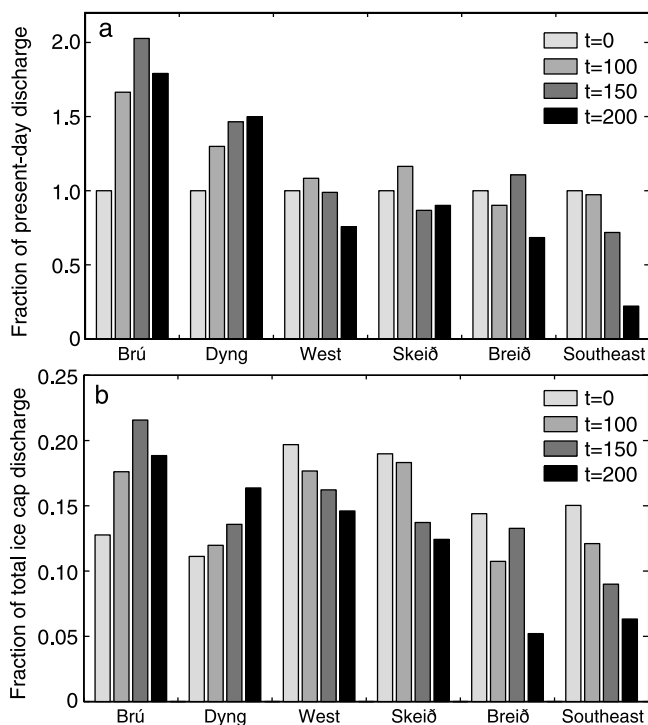
Figure 14. Simulated total discharge contributions from selected basins for 2°C per century warming and no change in precipitation. Each bar represents a particular time slice (see legend), and each bar cluster represents a particular drainage basin: Brú, Brúarjökull (A in Figure 2a); Dyng, Dyngjujökull (B in Figure 2a); West, Köldukvíslarjökull, Tungnaárjökull, and Síðujökull (C–E in Figure 2a); Skeid, Skeidarárjökull (F in Figure 2a); Breid, Breidamerkurjökull (G in Figure 2a); and Southeast, ice cap sector immediately east of Breidamerkurjökull. (a) Total (subglacial and groundwater) basin drainage normalized to the reference value ($t = 0$). (b) Fraction of total ice cap discharge routed through labeled basins.

minimal impact on Vatnajökull dynamics (Figure 15), due to the fact that Vatnajökull already has an abundant supply of water over the ice cap surface. This is in marked contrast to polar ice fields, which experience little or no melt in the accumulation areas. With very few exceptions, total simulated surface velocities decrease with glacier thinning (Figures 15a–15g). Surface velocity is the component sum of internal deformation and basal motion, where deformational velocities decrease with ice thinning.

[59] On the basis of the simulated basal velocity profiles (Figures 15h–15n), there is no evidence for a pronounced meltwater related acceleration. Köldukvíslarjökull exhibits the largest response (Figure 15j) in the form of a ~35% peak velocity increase from 0 to 100 years. Increases in basal velocity for the other outlet glaciers are small and are generally concentrated in the upper half of the profiles. The latter is indicative of a migration of the accumulation area toward the central divides and the increasing production of meltwater at high elevations. Thus areas formerly isolated from vigorous subglacial drainage experience meltwater enhancement of basal motion. For six of seven outlet glaciers, the simulated basal velocity profile at 100 years

exceeds the reference profile at some point well upglacier from the terminus; the 150 year profile does the same but further upglacier. In only one case (Figure 15i) does the 200 year profile exceed the 150 year profile at any point. Breidamerkurjökull (Figure 15n) experiences only very slight and short-lived increases in basal velocity.

[60] The sliding rule in (3) expresses basal motion as a function of both hydrology and driving stress. Driving stress decreases as the ice thins, so changes in basal motion in Figures 15h–15n reflect the competition of decreasing driving stress with generally increasing water pressures. From the general picture presented in Figure 15, it seems clear that the influence of hydrology on Vatnajökull dynamics cannot be further enhanced, implying that increased meltwater production would have only modest effects on measured velocity profiles. Breidamerkurjökull illustrates this point particularly well with its high simulated water production rates and the miniscule predicted acceleration (Figure 15n).

4. Summary and Conclusion

[61] Coupling models of ice dynamics and hydrology has enabled the most complete examination to date of Vatnajökull's sensitivity to a warming climate. The hydrology model requires geometric and mass balance input from the dynamics model, and in turn computes subglacial water pressure which is used in the parameterization of basal sliding. A reference climatology was defined based on spatially distributed 1961–1990 mean temperatures furnished by the Icelandic Meteorological Office and the only available map of precipitation. In order to remove model transients from our analysis, we conducted a 400 year preconditioning integration driven by estimates of the historical temperature record. Owing to uncertainty in the estimated temperatures over the ice caps, we introduce an offset to the reference temperature fields which we treat as a tuning parameter. Along with model parameter B_s, this offset is varied to achieve the best match between simulated and measured present-day ice cap volume and area. This procedure involves a number of important simplifications and assumptions.

[62] Future climate scenarios, with warming rates of 0°–4°C per century and 0–10% °C^{-1} rates of precipitation increase, were defined relative to the reference climate and applied to the preconditioned model. Simulations holding the reference climate fixed yield a relatively stable ice cap, with slight but monotonic decreases in volume and area over the 200 year period of investigation. For applied warming rates ≥2°C per century, ice cap volume and area reductions of 50% occur within 200 years for all precipitation scenarios. Guided by NCAR-CCSM simulations, we focus our attention on the results of 2°C per century warming with no change in precipitation. This prescribed climate produces outlet glacier retreat of several kilometers over 100 years, highest for Breidamerkurjökull and lowest for the northern outlets. For the same applied warming, retreat rates increase two to four times between 100 and 200 model years, resulting in a total recession of ~10 km for the northern and northwestern outlets, ~20 km for the western and southwestern outlets, and >25 km for Breidamerkurjökull.
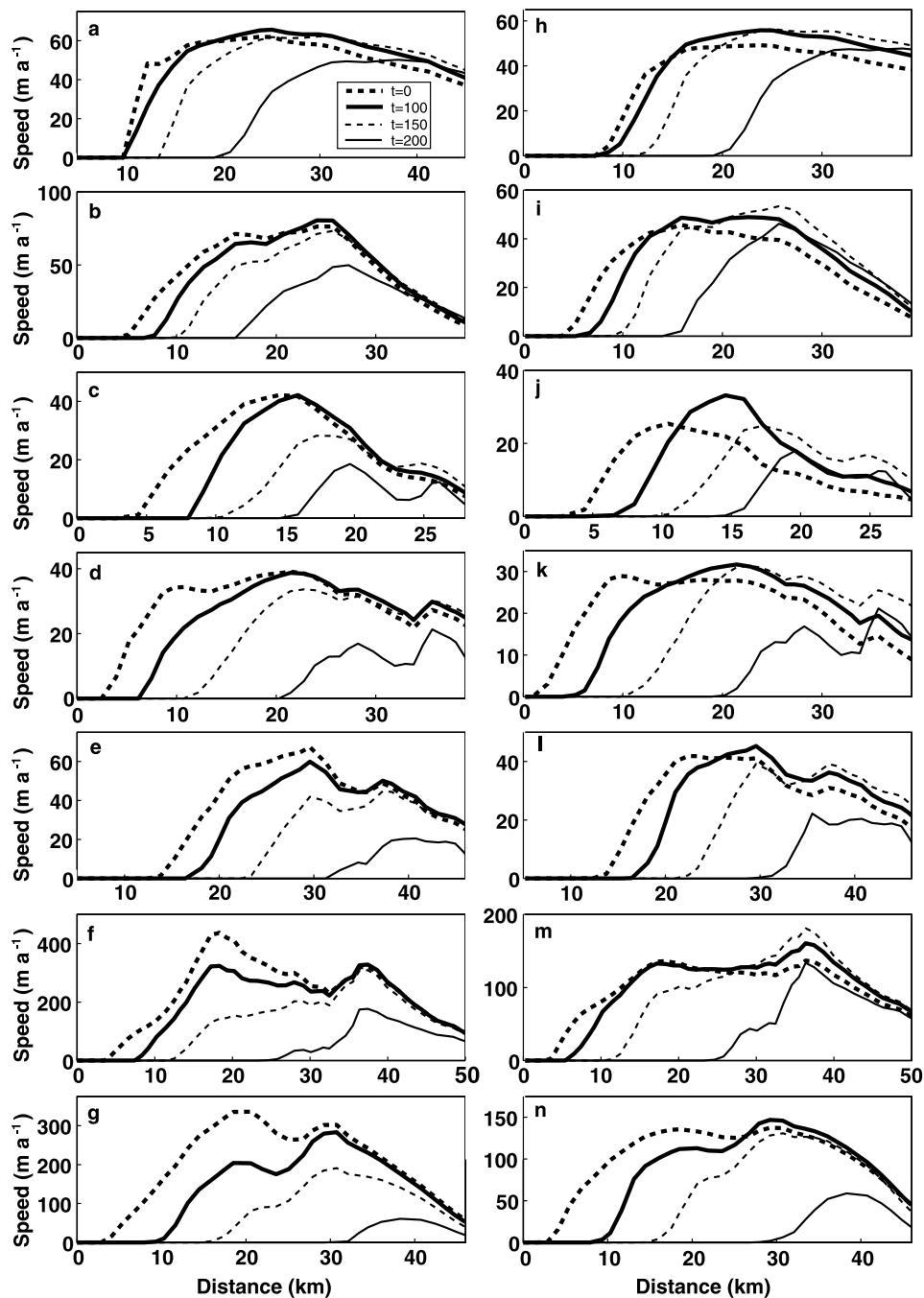
Figure 15. Simulated velocity profiles for 2°C per century warming and no change in precipitation. Profiles correspond to those in Figure 2a. (a–g) Surface velocity (deformation plus basal flow). (h–n) Basal flow velocity.

[63] The evolution of drainage under Vatnajökull, on the timescales presented here, is a consequence of changes in glacier geometry and mass balance. Changes in the distribution and magnitude of surface ablation and rain translate directly into changes in water input to the glacier bed. The net mass balance and the three-dimensional velocity structure dictate ice cap geometry, which largely controls the direction of subglacial water flow. For 2°C per century warming and no change in precipitation, glacier-derived runoff including subglacial and groundwater sources peaks at 25% above the reference value after 130 years. Discharge

maxima are higher and occur earlier for more rapid warming, with 4°C per century warming producing a discharge maximum >50% higher than the reference value after 100 years.

[64] Most of the rivers used in hydroelectric projects originate on the northern and western flanks of Vatnajökull. The northern river basins appear to be the most robust to climate change owing to their distance from warm coastal conditions, their higher elevations, and in the case of Dyngjujökull, its proximity to Bárdarbunga ice dome and favorable hypsometry. Discharge from Brúarjökull experi-

ences the greatest fractional increase of all river basins for 2°C warming per century and emerges as the dominant drainage basin after 100 years. Dyngjujökull is the only basin to experience a monotonic increase in discharge over the entire 200 year simulation period. After 200 years, it follows Brúarjökull in transporting the highest fraction of runoff from Vatnajökull. Discharge from the western basins, as well as from Skeidarárjökull and Breidamerkurjökull, fluctuates with climate warming but after 200 years is significantly lower than the reference value. Only the southeast sector of the ice cap undergoes a monotonic decline in discharge through the entire simulation period.

[65] Should Vatnajökull undergo the type of retreat suggested by these simulations, the implications for its drainage and periglacial hydrology could be substantial. Of the major outlet glaciers, Breidamerkurjökull exhibits the most dramatic geometric response to climate warming. Retreat of the southern outlet Skeidarárjökull will likely result in disturbance of jökulhlaup routing and frequency from subglacial lake Grímsvötn. Both of these outlets will support new or enlarged proglacial lakes as they retreat. While the northern and northwestern outlets of Vatnajökull appear to fare better under climate warming, individual rivers will be affected by drainage rerouting manifest as both sudden increases and decreases in discharge.

[66] Thinning ice increases the influence of bedrock topography on basal water drainage, which in areas such as the margin of Tungnaárjökull and western Brúarjökull, results in surface runoff being diverted from one river basin to another with only moderate retreat of the glacier margin. There are at least four rivers (Jökulsá á Fljótsdal, Kreppa/ Kverká, Skjálfandafljót, Tungnaá) that may be subject to this outcome within 200 years with 2°C per century warming. Rivers originating from western Vatnajökull would continue to be fed by groundwater. The southeastern flank of Vatnajökull appears to be susceptible to retreat across a margin-parallel bedrock ridge which would effectively isolate settlements on the southeast coast of Iceland from glacier-derived runoff. The sensitivity of Vatnajökull's periglacial hydrology to climate change mirrors the climate vulnerability of its outlet glaciers and is an expression of the unique control ice cap geometry exerts on subglacial water routing.

Appendix A: Model Preconditioning

[67] In order to define a reference model, provide some measure of model validation and remove transient artifacts from our future climate simulations, we drive the model through a 400 year variable climate preconditioning. While the characteristic response time of Vatnajökull should be much shorter than 400 years [Adalgeirsdóttir, 2003], we choose a period long enough that the result is insensitive to initial ice geometry. We restrict the period to 400 years because the climate record is much less certain prior to the year 1600. Using the spatial distributions of temperature in Figures 3a and 3b, combined with historical temperature estimates and measurements, we construct a plausible climate history for Vatnajökull from 1600 to 2000. In the absence of historical precipitation records, we use the reference precipitation field (Figure 3c) as representative of historical precipitation.

[68] Regular temperature measurements have been made since 1823 in Stykkishólmur, west Iceland, providing time series of the mean annual and July temperatures during this period. We smooth these records with an 11 year running mean and take the resulting time series to represent the historical variability of these two temperature quantities across Iceland. Temperature estimates prior to 1823 have been made by Bergthórsson [1969] based on sea ice distribution and other more subjective metrics. Assuming that the variability represented in his estimates applies to both annual and July temperatures, we construct time series representing mean annual and July temperature variability from 1600. We splice the estimates of Bergthórsson [1969] (from 1600 to 1950) with the measurements from Stykkishólmur (from 1823 to 2000) by shifting the time series to match their respective means during the period of overlap (1823–1950). In order to express the resulting time series as temperature anomalies relative to 1600, we subtract the smoothed temperature at 1600 from both the mean annual and July records (Figure 4a).

[69] The model is initialized at 1600 with present-day ice cap geometry. Accordingly, we assume that the temperature fields appropriate for 1600 can be expressed as perturbations to the reference temperature fields $T_{ann}^{ref}(x, y)$ and $T_{jul}^{ref}(x, y)$:

$$T_{ann}(x,y,1600) = T_{ann}^{ref}(x,y) - 0.65 \qquad (A1)$$

$$T_{jul}(x,y,1600) = T_{jul}^{ref}(x,y) - 0.28, \qquad (A2)$$

where 0.65°C and 0.28°C are, respectively, the mean annual and July temperature anomalies (Figure 4a) averaged over the period 1961–1990 (defined as the reference). This provides a consistent means of relating the reference temperature fields to those appropriate for 1600. We treat ΔT_{ann} in (11) as unknown and vary it jointly with parameter B_s in (3) to produce a simulated ice cap in best agreement with the data. The result of this exercise furnishes a reference model and an adjusted 1961–1990 climatology.

[70] To summarize, the model preconditioning assumes the following: (1) the reference temperature fields in (11) and (12), derived from interpolated data provided by the Icelandic Meteorological Office, represent valid corrected temperatures for the period 1961–1990, (2) the reference temperature fields represent valid spatial distributions of relative temperature for the period 1600–2000 (and indeed into the future); (3) mean annual and July temperature anomalies can be represented by the same proxy record prior to 1823 (Figure 4a); (4) the composite record in Figure 4a is an adequate representation of historical temperature variability in the vicinity of Vatnajökull; (5) 1961–1990 mean annual and July temperature anomalies (Figure 4a) can be subtracted from the respective 1961–1990 reference temperature fields to represent mean annual and July temperatures in 1600 as in (A1) and (A2); and (6) the present-day precipitation field provides a reasonable estimate of historical precipitation. Of these assumptions, (4) and (6) are likely to be the most problematic. Assumption (4) is threatened by the possibility that climate conditions were controlled by different circulation regimes

between west Iceland, where the measurements were collected, and southeast Iceland, where Vatnajökull is located. We make assumption (6) out of necessity, but precipitation patterns and amounts are certain to have varied over the last 400 years.

References

Adalgeirsdóttir, G. (2003), Flow dynamics of Vatnajökull ice cap, Iceland, Ph.D. thesis, 178 pp., ETH-VAW, Zürich, Switzerland.

Adalgeirsdóttir, G., G. H. Gudmundsson, and H. Björnsson (2000), The response of a glacier to a surface disturbance: A case study on Vatnajökull ice cap, Iceland, *Ann. Glaciol.*, 31, 104–110.

Adalgeirsdóttir, G., G. H. Gudmundsson, and H. Björnsson (2003), A regression model for the mass balance distribution of the Vatnajökull ice cap, Iceland, *Ann. Glaciol.*, 37, 189–193.

Bergthórsson, P. (1969), An estimate of drift ice and temperature in Iceland in 1000 years, *Jökull*, 19, 94–101.

Björnsson, H. (1974), Explanation of jökulhlaups from Grímsvötn, Vatnajökull, Iceland, *Jökull*, 24, 1–23.

Björnsson, H. (1982), Drainage basins on Vatnajökull mapped by radio echo soundings, *Nord. Hydrol.*, 4, 213–232.

Björnsson, H. (1986a), Surface and bedrock topography of ice caps in Iceland, mapped by radio echo-sounding, *Ann. Glaciol.*, 8, 11–18.

Björnsson, H. (1986b), Delineation of glacier drainage basins on western Vatnajökull, *Ann. Glaciol.*, 8, 19–21.

Björnsson, H. (1988), *Hydrology of Ice Caps in Volcanic Regions*, 139 pp., Soc. Sci. Islandica, Univ. of Iceland, Reykjavik.

Björnsson, H. (1996), Scales and rates of glacial sediment removal: A 20 km long and 300 m deep trench created beneath Breidamerkurjökull during the Little Ice Age, *Ann. Glaciol.*, 22, 141–146.

Björnsson, H. (1998), Hydrological characteristics of the drainage system beneath a surging glacier, *Nature*, 395, 771–774.

Björnsson, H. (2002), Subglacial lakes and jökulhlaups in Iceland, *Global Planet. Change*, 737, 255–271.

Björnsson, H. (2003), The annual cycle of temperature in Iceland, *Tech. Rep. 03037*, 44 pp., Icelandic Meteorol. Off., Reykjavik.

Björnsson, H., and P. Einarsson (1991), Volcanoes beneath Vatnajökull, Iceland: Evidence from radio echo-sounding, earthquakes and jökulhlaups, *Jökull*, 40, 147–168.

Björnsson, H., F. Pálsson, M. T. Gudmundsson, and H. H. Haraldsson (1998), Mass balance of western and northern Vatnajökull, Iceland, 1991–1995, *Jökull*, 45, 35–58.

Björnsson, H., F. Pálsson, and S. Gudmundsson (2001), Changes in the proglacial lake Jökulsárlón, SW-Iceland, 1934–1998, *Jökull*, 50, 1–18.

Björnsson, H., F. Pálsson, O. Sigurdsson, and G. E. Flowers (2003), Surges of glacier in Iceland, *Ann. Glaciol.*, 36, 82–90.

Eythórsson, J., and H. Sigtryggsson (1971), *The Climate and Weather of Iceland*, vol. 1, *The Zoology of Iceland*, Ejnar Munksgaard, Reykjavik.

Flowers, G. E., and G. K. C. Clarke (2002a), A multicomponent coupled model of glacier hydrology: 1. Theory and synthetic examples, *J. Geophys. Res.*, 107(B11), 2287, doi:10.1029/2001JB001122.

Flowers, G. E., and G. K. C. Clarke (2002b), A multicomponent coupled model of glacier hydrology: 2. Application to Trapridge Glacier, Yukon, Canada, *J. Geophys. Res.*, 107(B11), 2288, doi:10.1029/2001JB001124.

Flowers, G. E., H. Björnsson, and F. Pálsson (2003), New insights into the subglacial and periglacial hydrology of Vatnajökull, Iceland, from a distributed physical model, *J. Glaciol.*, 49, 257–270.

Freeze, A., and J. A. Cherry (1979), *Groundwater*, 604 pp., Prentice-Hall, Upper Saddle River, N. J.

Geirsdóttir, Á., and J. Eiríksson (1994), Growth of an intermittent ice sheet in Iceland during the Late Pliocene and Early Pleistocene, *Quat. Res.*, 42, 115–130.

Gent, P. R., and G. Danabasoglu (2004), Heat uptake and the thermohaline circulation in the Community Climate System Model, Version 2, *J. Clim.*, 17, 4058–4069.

Glen, J. W. (1955), The creep of polycrystalline ice, *Proc. R. Soc. London, Ser. A*, 228, 519–538.

Gudmundsson, M. T., F. Sigmundsson, and H. Björnsson (1997), Ice-volcano interaction of the 1996 Gjálp subglacial eruption, Vatnajökull, Iceland, *Nature*, 389, 954–957.

Gudmundsson, S., H. Björnsson, F. Pálsson, and H. H. Haraldsson (2003), Comparison of physical and regression models of summer ablation on ice caps in Iceland, *Tech. Rep. RH-15-2003*, 31 pp., Sci. Inst. Univ. of Iceland, Reykjavik.

Gylfadóttir, S. S. (2003), Spatial interpolation of Icelandic monthly mean temperature data, *Tech. Rep. 03006*, 27 pp., Icelandic Meteorol. Off., Reykjavik.

Huybrechts, P., A. Letréguilly, and N. Reeh (1991), The Greenland Ice Sheet and greenhouse warming, *Palaeogeogr. Palaeoclimatol. Palaeoecol.*, 89, 399–412.

Intergovernmental Panel on Climate Change (2001), *IPCC Third Assessment Report: Climate Change 2001: The Scientific Basis*, edited by J. T. Houghton et al., 944 pp., Cambridge Univ. Press, New York.

Jóhannesson, T., O. Sigurdsson, T. Laumann, and M. Kennett (1995), Degree-day glacier mass-balance modelling with applications to glaciers in Iceland, Norway and Greenland, *J. Glaciol.*, 41, 345–358.

Kiehl, J. T., and P. R. Gent (2004), The Community Climate System Model, Version Two, *J. Clim.*, 17, 3666–3682.

Knudsen, Ó., and A. R. Russell (2002), Jökulhlaup deposits at Ásbyrgi, northern Iceland: Sedimentology and implications for flow type, *IASH Publ.*, 271, 107–112.

Letréguilly, A., N. Reeh, and P. Huybrechts (1991), The Greenland Ice Sheet through the last glacial-interglacial cycle, *Palaeogeogr. Palaeoclimatol. Palaeoecol.*, 90, 385–394.

Marshall, S. J., and G. K. C. Clarke (1997a), A continuum mixture model of ice stream thermomechanics in the Laurentide Ice Sheet: 1. Theory, *J. Geophys. Res.*, 102, 20,599–20,613.

Marshall, S. J., and G. K. C. Clarke (1997b), A continuum mixture model of ice stream thermomechanics in the Laurentide Ice Sheet: 2. Application to the Hudson Strait Ice Stream, *J. Geophys. Res.*, 102, 20,615–20,637.

Marshall, S. J., and G. K. C. Clarke (1999), Ice sheet inception: Subgrid hypsometric parameterization of mass balance in an ice sheet model, *Clim. Dyn.*, 15, 533–550.

Marshall, S. J., L. Tarasov, G. K. C. Clarke, and W. R. Peltier (2000), Glaciological reconstruction of the Laurentide Ice Sheet: Physical processes and modeling challenges, *Can. J. Earth Sci.*, 37, 769–793.

Payne, A. J. (1995), Limit cycles in the basal thermal regime of ice sheets, *J. Geophys. Res.*, 100, 4249–4263.

Reeh, N. (1991), Parameterization of melt rate and surface temperature on the Greenland Ice Sheet, *Polarforschungen*, 59, 113–128.

Sigmundsson, F. (1991), Post-glacial rebound and asthenosphere viscosity in Iceland, *Geophys. Res. Lett.*, 18, 1131–1134.

Sigmundsson, F., and P. Einarsson (1992), Glacio-isostatic crustal movements caused by historical volume change of the Vatnajökull ice cap, Iceland, *Geophys. Res. Lett.*, 19, 2123–2126.

Sun, S., and J. E. Hansen (2003), Climate simulations for 1951–2050 with a coupled atmosphere-ocean model, *J. Clim.*, 16, 2807–2826.

Thorarinsson, S. (1958), The Öræfajökull eruption of 1362, in *Acta Naturalia Islandica, Icelandic Inst. of Nat. Hist. Monogr. Ser.*, vol. 2, 100 pp., Icelandic Inst. of Nat. Hist., Reykjavik.

Thorpe, R. B., J. M. Gregory, T. C. Johns, R. A. Wood, and J. F. B. Mitchell (2001), Mechanisms determining the Atlantic thermohaline circulation response to greenhouse gas forcing in a non-flux adjusted coupled climate model, *J. Clim.*, 14, 3102–3116.

Tómasson, H. (1973), Hamfarahlaup í Jökulsá á Fjöllum, *Nátturufrædingurinn*, 43, 12–34.

————————

H. Björnsson, Science Institute, University of Iceland, Dunhaga 3, 107 Reykjavík, Iceland. (hb@raunvis.hi.is)

G. K. C. Clarke, Department of Earth and Ocean Sciences, University of British Columbia, Vancouver, BC, Canada V6T 1Z4. (gclarke@eos.ubc.ca)

G. E. Flowers, Department of Earth Sciences, Simon Fraser University, 8888 University Drive, Burnaby, BC, Canada V5A 1S6. (gflowers@sfu.ca)

S. J. Marshall, Department of Geography, University of Calgary, Calgary, AB, Canada T2N 1N4. (marshals@ucalgary.ca)